Project title:
Development of sensor-based Citizens' Observatory Community for improving quality of life in cities
Acronym: **CITI-SENSE** Grant Agreement No: **308524**
EU FP7- ENV-2012
Collaborative project

Deliverable D8.5

Final sensor platform report: Final description and assessment of the performance of the sensor platforms

Work Package 8

Date: 16.11.2016

Version: 1.0

Leading Beneficiary:	TECHNION - ISRAEL INSTITUTE OF TECHNOLOGY
Editor(s):	Alena Bartonova, Sonja Grossberndt (NILU)
Author(s) (alphabetically):	David Broday, Yael Etzion, Barak Fishbain (TECHNION)
Dissemination level:	Public

Versioning and contribution history

Version	Date issued	Description	Contributors
V1ti2	06.09.2016	Ver 1 – Technion iteration 2	D.B., Y.E., B.F.
VF1	17.11.2016	Ver 1 – Final revision after internal review 1 and 2	Leonardo Santiago

Peer review summary

Internal review 1			
Reviewer	Núria Castell (NILU)		
Received for review	30.10.2016	Date of review	08.11.2016

Internal review 2			
Reviewer	Arne Berre (SINTEF)		
Received for review	30.10.2016	Date of review	11.11.2016

Executive Summary

Accurate evaluation of air pollution on public health and human-wellbeing requires high-resolution measurements. Standard air quality monitoring stations provide accurate pollution levels but due to their sparse distribution (which is derived from their cost and deployment requirements) they cannot capture the highly resolved spatial air pollution variations within cities. Similarly, dedicated field campaigns that use tens or even hundreds of measurement devices and obtain highly dense spatial coverage are deployed for relatively short periods of no more than 2-3 weeks per season. Nowadays, advances in communication and sensory technologies enable the deployment of dense grids of wireless distributed air quality monitoring nodes, yet their ability to capture the spatiotemporal pollutant variability at the sub-neighbourhood scale has never been thoroughly tested. The low power consumption and small size of typical nodes that can build a wireless distributed sensor network (WDSN) enable both stationary as well as mobile sensing, and of deployment of single or multiple nodes simultaneously (i.e. in redundancy). Yet, the most important promise of WDSN is in their unprecedented potential to become a tool for studying many environmental processes, and to open a new era for public engagement and participation in scientific work. This report summarizes many efforts performed within the EU FP7 CITI-SENSE project to study the feasibility and the required methods (experimental, computational and theoretical) to use data streams from this technology, and to assess and tune the results for different possible stakeholders, according to the quality of the sensor data and based on the application that the user seek.

This report summarizes work done by numerous project partners. Field calibration studies were done in nine cities across Europe (Barcelona, Belgrade, Cambridge, Edinburgh, Haifa, Ljubljana, Oslo, Ostrava, Vienna). Eight cities deployed air quality sensor platforms as part of empowerment initiatives (Barcelona, Belgrade, Edinburgh, Haifa, Ljubljana, Oslo, Ostrava, Vienna).

We report findings on two sensor technologies (metal-oxide and electrochemical sensors); four stationary platforms (AirBase, CVUT, DNET, AQMesh), with only the AQMesh platform chosen by the project to continue to the last phase of the project, which involved field deployment of the sensor nodes; two mobile/personal platforms (ATEKNEA, JSI), with only the ATEKNEA LEO platform chosen by the project to continue to the last phase of the project, which involved field testing; six pollutants (CO, NO, NO_2, O_3, PM, TVOC) and 3 other environmental parameters: ambient temperature (T), relative humidity (RH) and noise; two modes of use of such a technology (stationary wireless distributed sensor network, WDSN, and personal/ mobile sensor nodes). Based on a comprehensive evaluation, only a subset of technologies was used for large scale field deployment; the types and numbers deployed are below (starred units were only used in the pilot study). In addition to those, also ten DNET sensor units were part of the main field deployment in Belgrade.

Location/Provider	GEOTECH (WP2)	ATEKNEA (WP2)	ATMOS (WP3)	OBEO (Radon)
Barcelona (BCN)	25 + 5*	11	-	-
Belgrade (BEL)	25	11	12	4
Edinburg (EDI)	24	11	12	4
Haifa (HFA)	24	11	-	-
Ljubljana (LJU)	12 + 6*	11	12	4
Oslo (OSL)	24	11	12	4
Vienna (VIE)	24	11	-	-
Ostrava (OSR)	16	9	-	-
Total	**174**	**86**	**48**	**16**
Total of 324 units				

Through a meticulous testing by different partners (i.e. independent testing) in different geographic locations and for different periods and seasons (i.e. meteorological and climatological conditions), we evaluated the capability of the networks to capture spatiotemporal concentration variations in the

laboratory, during collocation studies, and during real urban-scale deployment. In general, **we found an exceptional response that can shade light on fine spatiotemporal variability of the pollutant concentrations**, both intra-urban (within a city) and inter-urban (across cities). In particular, we show that **it is possible to identify intra-urban pollutant "hot-spots"**. The similarity among the concentration patterns during weekends across urban areas and the variability during weekdays further support our conclusion that the sensor are sensitive enough to capture air pollution patterns and respond rather instantaneously to their microenvironment changing conditions, although their response may suffer from interference with many other environmental factors rather than reflecting only the nominal pollutant concentrations.

We also found and highlight numerous limitations of the current sensor (and platform) technology, which require careful thinking and much development before it could find its way in use for applications and by stakeholders that require accurate and reputable absolute values. It is noteworthy that unfortunately, the most promising sensor technology at present for measuring fine particle number concentrations is the one that the project as a whole considered the least (due to great development of this technology since the project has been proposed and launched). However, for applications that require or may suffice with relative pollutant levels, either in time or space or both, we provide a detailed account of the capabilities of the sensor technologies, and the maintenance they require. The latter include administrative maintenance (battery replacement, faulty sensor replacement, etc.) as well as repeated calibrations. Thus, apart from the classical laboratory calibration against high-end instrumentation and under fully controlled conditions, which is reported here to be insufficient for the technology at hand and for the different applications it is required to address, we report here three different field calibration procedures (while the sensor nodes are collocated and two variations while the nodes are deployed in their required measurement sites – i.e. *in-situ* calibration approaches). Moreover, we carefully describe (and refer to) algorithms developed as part of this work, which are general and can be used by other researchers that work on similar problems as well as in the future, when improved sensing technology will emerge. In general, all the calibration methods have been evaluated in great detail and in various ways, using the rich data the WDSN supplies in both space and time. Field calibration has been found essential, and is shown to improve the network performance tremendously. Overall, our results support the compatibility of WDSN for measuring urban air pollution at a sub-neighbourhood spatial resolution, and to suit the requirement for highly spatiotemporal resolved measurements at the breathing-height. The accuracy and repeatability of the measurements dictate certain applications, especially if non-professional users are to use it and its data. In particular, the current state of this technology does not fit the requirements of regulatory agencies, as well as cannot provide reliable (absolute) exposure estimates of urban air pollution, to be used in epidemiological studies. However, they have numerous applications in education and in citizen science, and for raising the public awareness to air pollution as part of a citizen observatory allegiance.

Typically, the accuracy of WDSN devices is assessed by reporting the mean error (ME) or correlation coefficients with respect to laboratory equipment. However, these criteria do not account for the sensors' performance during their field deployment and, in fact, may not suit (e.g. be too conservative) many possible applications for this new technology for which accurate measurement are not a must, but for which either precision or even just pollution trends are sufficient. For this reason, we developed and present a comprehensive Sensor Evaluation Toolbox (SET), which enable evaluation of the WDSN technology based on a range of criteria, so that their performance for a variety of applications can be assessed. The SET contains four not commonly used evaluation criteria that examine the sensors' reliability, ability to locate pollution sources, capability to represent pollution at a coarse scale, and competency to capture the temporal variability of the observed pollutants. We demonstrate the application of this toolbox on measurements acquired by WDSN node across the whole Europe, during

different time periods and seasons, and for different pollutants. We showed that the SET facilitates a comprehensive across-platform analysis of the sensor performance envelope and desired working conditions. Moreover, apart from calibration needs and the benefit of (some) redundancy in WDSN data collection, we also addressed within the project the effect of airflow on the sensor readings, be it the effect of the varying wind field or of the ego-motion of mobile nodes either worn (personal nodes) or mounted on vehicles or carried while cycling (mobile nodes). The impact of sensor motion on its performance was clearly shown, and attributed mainly to the air velocity at the sensor face, since the sensors are inherently designed to measure under diffusive rather than convective regime. This has skipped almost all previous studies that used similar nodes for measurement while on motion. In general, while low-cost platforms present low accuracy for regulatory purposes they can provide relative and aggregated information about the observed air quality.

Table of Contents

Introduction

Recent developments in sensory and communication technologies have made the deployment of portable and relatively low-cost Micro Sensing Units (MSUs) possible. These MSUs operate as a set of standalone nodes, where each node houses several sensors for different air pollutants, thus forming a Wireless Distributed Environmental Sensor Network (WDSN). Numerous individual nodes enable to gather high-resolution spatial and temporal data and therefore allow for a better interpolation and the generation of dense pollution maps, which are closer to real-life pollution dispersion scenarios (Kanaroglou et al., 2005). The gaseous sensors mounted on these MSUs are low-power and low-cost, and are based on widely understood amperometric sensor methodologies designed for sensing selected gases at the parts-per-million (ppb) level. Electronic circuitry, which applies signal processing, allows for the detection at the part-per-billion (ppb) level (Mead et al. 2013). Recent miniaturization of Optical Particles Counters (OPCs) and solid state sensors allows to extend the MSUs capabilities to measure particulate matter (PM) as well.

The main goal of **WP2 Empowerment Initiative 1 - Urban Quality** was to empower citizens by providing them with quantitative information about the air pollution they are exposed to, through a wireless distributed sensor network (WDSN) that measures pollutants relevant to the urban air quality. Data for indoor and public spaces were also part of the study, this was the goal of **WP3 Empowerment Initiative 2 (Schools) & 3 (Public Spaces)**.

In order to provide WP2 and WP3 empowerment initiatives with the sensor technology, different platforms were applied, including stationary and mobile personal units, back to back with ongoing testing and evaluation of the units in the framework of **WP8 Methods - Sensor platform**. Most resources (time, person month, money) of WP8 were invested in development of the static nodes, which were expected to enable continuous measurements for long time. Partners involved in development of the stationary sensor platform were Environmental Instruments Ltd. (UK), AIRBASE (Israel), Alphasense provided Atmospheric Sensors platform (UK), DNET (Serbia), CVUT (Czech Rep.), and OBEO (Norway). Partners involved in the development of the mobile sensor platforms include ATEKNEA (Spain) and JSI (Slovenia). A second broader task of WP8 was to evaluate the measurements. Laboratory calibration, validation and approval tests of the individual sensors were conducted by the sensor manufacturer (ALPHASENSE, UK), followed by evaluation of the sensor platforms in laboratory conditions (NILU, NO), and in extensive field campaign (Technion, Israel; NILU, NO; Vinca, Serbia and UCAM, UK). Further evaluation has been done by all the case study cities (Barcelona, Edinburgh, Ostrava, Oslo, Belgrad, Haifa, Vienna, Ljubljana). Data streaming from the WDSN developed within WP8 was planned to supplement data from existing air monitoring station networks and to enable development of near-real-time models (e.g. land-use regression, data assimilation, etc.). Essentially, WP8 addressed two different data models. The first model is pollution maps based on stationary nodes measurements that can be used for tracking the exposure of individuals along their personal routes, according to personal GPS tracking (e.g. by personal smartphone). The pollution maps are updated according to data sent by the static nodes to the CITI-SENSE server via GPRS communication on a sub-hourly basis. Alternatively, personal mobile nodes were developed with the intention to enable people monitor their proximate environment and transport the measurements in real-time (via Bluetooth) to a portal that will link their measurements and trajectories and provide personal report. Moreover, the personal sensors were expected to collect also data on the physical activity (PA) in which the individual is engaged, and enable analysis based on PA patterns.

Following careful and informed discussion, the static electrochemical-sensor based nodes were agreed to contain sensors for the following pollutants: NO, NO_2, CO, O_3 (and PM in a later phase), as well as for temperature, humidity and noise. The metal oxide-sensor based nodes were agreed to contain sensors for the following pollutants: NO_2, TVOC, O_3, TSP (and NO in a later phase), as well as for temperature, humidity and noise. The nodes were designed to be mounted in a fixed location

outdoors. The personal electrochemical-sensor based nodes were agreed to contain sensors for the following pollutants: NO_2, NO, O_3, as well as for temperature and relative humidity.

Moreover, it was clear that the user will need to communicate with the collected data through an app that will facilitate the process and expose the user to data which will be "cleared" by the project partners (accounting for the quality of the data and for privacy issues). The app for the stationary nodes was agreed to be developed by **WP6 Methods - Information products and services** (by NILU and DNET) whereas the app for the personal nodes was developed within WP8 (by ATEKNEA). This task required some preliminary work on the app design as well as agreement on its content, as will be described below.

Considerations for a favourable platform selection

Mobile measurements provide better spatial coverage at the expense of lower temporal resolution in each location (e.g., Sabaliauskas et al., 2014; Hasenfratz et al., 2014), yet sensor vibrations during the measurement may lead to artifacts (Cai et al., 2013). On the other hand, stationary sensors provide better temporal extent and resolution per location (e.g. Yu et al., 2016). Hence, this was the preferable choice, given the need for frequent field calibration and given the logistical advantage (easier to handle and maintain). Studying the effect of mobility-driven wind gusts on the MSU sensors' readings during phase I (Lerner et al., 2015) further supported our choice to concentrate in phase II (as of M24 of the project timeline) on static deployment based on electrochemical sensors in a platform that requires minimal maintenance, using internal power battery and cellular communication.

Brief summary of phase I results

In phase I (M1-24) of the study, Technion examined the AirBase platform with the metal oxide (MO) chemoresistive sensors for O_3, NO_2 and total volatile organic compounds (TVOC), testing the suitability of such a sensor network for measuring pollutant levels and for capturing their spatiotemporal concentration variability. Another aim was to develop a reliable field calibration procedure for the sensors (Moltchanov et al., 2015). To test the sensors' response to different microenvironments at a neighborhood scale with respect to their sensitivity and detection range, we deployed six MSUs at three different locations in the Haifa study area (two units per site), some 100–150 m apart, during summer 2013 (71 days). Overall, the correlations of the collocated units (with an AQM) ranged between 0.92–0.99 for O_3, 0.77–0.99 for TVOC and 0.78–0.98 for NO_2. In contrast, low correlations were found between concentrations of both NO_2 and TVOC measured by WDSN nodes placed at AQMs outside the Haifa study area, indicating that the measured concentrations echoed to some extent local conditions, and responded to the specific microenvironment where the nodes were placed. Diurnal patterns of NO_2 concentrations among collocated nodes were also similar. In particular, after every rotation of the nodes between different AQM locations the NO_2 sensors successfully adjusted to their new microenvironments and measured similar and site-distinct diurnal patterns, comparable to those measured by the previously collocated nodes (stationary measurements). The diurnal and weekly patterns of TVOC concentrations that were measured near a busy road were very similar to those of the NO_2, suggesting that the TVOC sensors are sensitive to traffic-related pollution. Indeed, the reported range of urban CO concentrations (Mead et al., 2013; Carotta et al., 2001) suggested that readings of the TVOC sensor were mostly due to ambient CO. In spite of the encouraging results, field calibration of the NO_2 (e.g. through collocation at the AQM site) could not be performed, mainly because of low ambient concentration of NO_2 in the AQM site to meet the detection range (< 10 ppb during the study period, whereas the sensor detection range was 10–2000 ppb with 5 ppb sensitivity). Calibration of TVOC sensors (to CO equivalent values) was not possible, as there were no reference CO measurements at the required range and resolution. Ozone concentrations, although highly correlated among collocated nodes, suffered from considerable inter-nodal variation, unlike the marginal inter-nodal variation of NO_2 and TVOC among collocated nodes. This inconsistency results from nodal-

specific gain and bias that characterize the low-cost MO O_3 sensors. Using linear regressions to adjust the nodes' measured O_3 values to collocated AQM measurements improved considerably the inter-nodal measurement consistency, with the mean absolute error between the nodes decreasing from 4.3–17.1 ppb to 3.2–6.2 ppb (Moltchanov et al., 2015). Yet, the individual nodes' gain and the bias coefficients were found to change significantly over time. The temporal change of the regression coefficients can be attributed to aging of the sensors, resulting in alterations in the gain (Williams et al., 2013), and to episodic events, such as rain and dust storms, that cause dirt to accumulate on the sensors. The sensor-specific temporal variation of the calibration parameters resulted in a non-linear inter-nodal (i.e. relative) divergence of the readings and called for a frequent field calibration of all the nodes. Since frequent collocation of the WDSN nodes with an AQM station is many times impractical, an in-situ night-time calibration procedure has been suggested. Urban O_3 concentrations during nighttime are rather spatially homogenous whereas during the day they reveal considerable spatial variability, resulted by traffic related variability of emissions of nitrogen oxides and volatile organic compounds across the neighborhood. Therefore, calibration coefficients for each day were calculated based on AQM data from 1:00-4:00 am of the three preceding days (Moltchanov et al., 2015). This rolling forwards field calibration procedure reduced the average mean absolute deviation between collocated WDSN O_3 measurements from 3.7-18.7 ppb to 0.5-1.1 ppb, and enabled revealing the spatial variability of daily O_3 concentrations. Yet, this calibration concept is relevant only when the pollutant concentrations exhibit negligible spatial variability for a sufficiently long period, and when the true concentrations are above the sensors' detection limit. Unfortunately, this criterion did not hold for NO_2 in the Haifa residential case study, as well as in many other urban areas.

Phase II sensor units

Based on the work performed in phase I of the project, in phase II the project decided to continue using stationary and personal nodes for outdoor air quality monitoring from only one provider for each type of nodes: Environmental Instruments Ltd. supplied the stationary WDSN nodes and ATEKNEA provided the personal WDSN nodes. Hence, we describe here in more detail only these nodes. For indoor air quality monitoring we employed the platform provided by Atmospheric Sensors, which included sensors for CO, NO, NO_2, Total VOC, O_3 and CO_2.

2. Static Platform Providers

ATMOSPHERIC SENSORS

Atmospheric sensors provided the units through its partner ALPHASENSE. The units were designed as stationary platforms for indoor measurements. They were not weather-proof and worked on mains supply. They measured six gaseous components (carbon monoxide, nitric oxide, ozone, nitric dioxide, total volatile organic compounds and carbon dioxide) as well as temperature, relative humidity and atmospheric pressure. An integrated optical particulate counter and a noise sensor were also available on these units. Table 1 provides information on the system gas sensing devices. An integrated GPRS modem regularly sends data to Atmospheric Sensors server. Collected data were available as Excel files on a FTP site.

Table 1. Atmospheric Sensors node gas sensing specifications

Gas	**CO**	**NO**	**NO_2**	**O_3**	**Tot VOC**	**CO_2**
Sensor technology	Electrochem.	Electrochem.	Electrochem.	Electrochem.	PID	NDIR
Measuring range	n.a	n.a	n.a	n.a	n.a	n.a
Sensor provider	Alphasense	Alphasense	Alphasense	Alphasense	Alphasense	Alphasense
Sensor type	CO-A4	NO-A4	NO2-A42F	OX-A421	PID-AH	IRC-AT

DunavNET

The Dunavnet (DNET) units measured six gaseous components (carbon monoxide, nitric oxide, ozone, nitric dioxide and carbon dioxide) as well as temperature, relative humidity and atmospheric pressure. Table 2 presents the specifications of the system sensors. An integrated GPRS modem allowed data transfer to Dunavnet's server. Data were available on a dedicated web-site.

Table 2. DunavNet unit gas sensor specifications

Gas	**CO**	**NO**	**NO_2**	**O_3**	**CO2**
Sensor technology	Electrochemical	Electrochemical	Electrochemical	Electrochemical	Electrochemical
Measuring range	0-5000 ppb	0-2000 ppb	0-200 ppb	0-200 ppb	0-200 ppb
Sensor provider	Alphasense	Alphasense	Alphasense	Alphasense	Alphasense

AQMesh

Environmental Instruments Ltd AQMesh nodes are battery operated stationary platforms that measure four gaseous components (CO, NO, NO_2 and O_3) and the total particle count (as an integration over 32 particle size channels). PM_{10} and $PM_{2.5}$ are estimated by converting the particle counts into PM mass-based fractions assuming a spherical particle shape and standard density. A proprietary algorithm is used to post-process the data gathered by the gas sensors, aiming to correct for cross-interferences and for the effect of temperature and relative humidity. The AQMesh nodes measure

also temperature, relative humidity and atmospheric pressure. Table 3 and Table 4 present information on the platform and the sensors. In phase II of the project we used v3.5 AQMesh nodes. This version included an O_3-filtered NO_2 sensor that was supposed to efficiently reject O_3 and, hence, eliminate cross-sensitivity issues. Standard AQMesh nodes deliver one-hour averaged data but were configured to deliver 15 min averaged data. An integrated GPRS modem allowed data transfer to the AQMesh database server. The data were available through a dedicated website.

Table 3. AQMesh gas sensor specifications

Gas	**CO**	**NO**	**NO_2**	**O_3**
Sensor technology	Electrochemical	Electrochemical	Electrochemical	Electrochemical
Measuring range	0-5000 ppb	0-2000 ppb	0-200 ppb	0-200 ppb
Sensor provider	Alphasense	Alphasense	Alphasense	Alphasense
Sensor type	CO-B4	NO-B4	NO2-B42F	OX-B421

Table 4. AQMesh particle sensor specifications

Source	**Laser**
Method	Light scatter
Range	0.3 µm – 30 µm
Sensitivity	< 1µm
Counter performance	Max count rate 3.3 kHz (3333 counts/s) Zero count rate < 1/minute
Number of channels	32
Flow rate	0.5 litres/minute
Concentration limit	2 million / litre
Particle count range	0-1000 particles/cm^3
$PM_{2.5}$ range	0-500 µg/m^3
PM_{10} range	0-1000 µg/m^3
Sensor provider	AQMesh (Environmental Instruments Ltd)

AQMesh units have gone through several major modifications since the beginning of the project. The M12 pilot units were referred to as V3.0 by Environmental Instruments (previously, GEOTECH). The M24 units are referred to as v3.5 by Environmental Instruments Ltd. All test results displayed in this report were obtained with version V3.5 of the pods. The key differences between the two versions are:

- V3.0 - The original Alphasense NO_2 sensor did not separate NO_2 and O_3 well (unfiltered for O_3 and susceptible to multiple cross-gas effects). The O_3 sensor had similar problems.
- V3.5 - Driven by the O_3-filtered NO_2 sensor from Alphasense, as supplied around the end of 2014. This sensor was expected to provide a better performance, particularly in separation of NO_2 and O_3.

OBEO

The Obeo device is a stationary sensor package for measurement of radon concentration in indoor environment. Obeo requires a constant power supply. Radon is a source of alpha radiation and based on past experience, silicon PIN photodiodes have proven to be relatively cheap, highly effective alpha radiation detectors with very good detection characteristics. Because of that, within this device we have integrated silicon semiconductor detector for radon.

The device for radon measurement is equipped with a detector whose measurement resolution is 1 Bq/ m3. Operating temperature of the platform is in the range of 5-35 °C. The platform has a built-in GSM module with the following characteristics:

- 850-1900MHz GSM / EGSM / DCS / PCS.
- Radon sensor has a 1h time resolution of measurement. In addition to the GSM module, the instrument has a QUAD BAND antenna, which together with a GSM module enables the transfer of data from the sensors to the server. Data from the server are then further visualized on a dedicated web site. Site visualization can be accessed on the basis of IMEI number, which is located on the instrument. Thus, for each platform there is a different web address for measurements access.

Within the CITI-SENSE project activities, in the first iteration in Belgrade, we used first version of the Obeo platform. In the beginning, there was a problem with the transfer of data, but later the device established data flow. This platform was compared with screening method with activated carbon canister as passive sampler and it was found to have a satisfactory agreement with the Obeo sensor, particularly in area with higher radon concentration.

In the second phase of the CITI-SENSE project, three additional Obeo radon sensors with improved design were placed in Belgrade, but failed to establish a reliable data flow. Hence, further testing of the radon sensors was cancelled.

CVUT

The units measure four gaseous components (carbon monoxide, TVOC, sulphur dioxide and nitric dioxide) as well as temperature, relative humidity and atmospheric pressure. Table 5 presents the specifications of the sensors of the system.

Table 5. CVUT unit gas sensor specifications

Gas	**CO**	**NO_2**	**SO_2**	**Tot VOC**
Sensor technology	Electrochemical	Electrochemical	Electrochemical	PID
Sensor provider	Alphasense	Alphasense	Alphasense	Alphasense

AirBase

The CanarIT units measured as many as six gaseous components (carbon monoxide, carbon dioxide, nitric oxide, ozone, nitric dioxide and TVOC) as well as temperature, relative humidity and atmospheric pressure. A noise sensor was also available on these units. The original plan was to use two different configurations, one dedicated for outdoor use and one for indoor measurements. Table 6 presents the specification of the system sensors. An integrated GPRS modem allows data transfer to Airbase server. Data were available on a user-friendly dedicated web-site.

Table 6. Airbase CanarIT node gas sensing specifications

Gas	**CO_2**	**NO**	**NO_2**	**O_3**	**VOC**
Sensor technology	NDIR	Electrochemical	MOx	MOx	PID
Sensor provider	Alphasense	Alphasense	Applied sensors	Aeroqual sm50	Applied sensors

3 Mobile Platform Providers

ATEKNEA

LEO units from Ateknea (Little Environmental Observatory) are battery-driven mobile platforms. These compact units measure three gaseous components (carbon monoxide, ozone and nitric dioxide) as well as temperature, relative humidity and atmospheric pressure. Sampling rate can be defined by the user (as short as 5s). Table 7 displays specifications for its gas sensors. The unit is designed as a highly portable unit communicating in real-time with a smart-phone via Bluetooth. The necessary smart-phone app has been finalized during M36-48. A micro-USB output allows data transfer to a PC. Battery capacity allows 8-hour sampling runs. This is the second version of Ateknea's portable unit.

Table 7. Ateknea node gas sensing specifications.

Gas	**NO**	**NO_2**	**O_3**
Sensor technology	Electrochemical	Electrochemical	Electrochemical
Measuring range	n.a	n.a	n.a
Sensor provider	Alphasense	Alphasense	Alphasense
Sensor type	NO-A4	NO2-A42F	OX-A421

JSI

After finalizing the phase II sensor units VESNA-PAQ and the corresponding mobile app for collecting, displaying and forwarding measurement data to the Snowflake data platform in year 3, the only activity in year 4 of the project (periods M37-M42 and M43-M48) was provision of technical support to testing of units in the Ljubljana pilot and at empowerment activities.

4 Sensors Evaluation in the Laboratory

The laboratory study (performed by NILU, NO) evaluated the performance of the sensors against traceable gas standards under reproducible and accurately contolled ambient conditions.

The testing set-up was built around three separate exposure chambers made of Pyrex glass. Figure 1 shows a rough schematic presentation of the system, including one chamber only for the sake of simplicity. All parts of the pneumatic circuit between the gas generation component and the chamber outputs were made of either PTFE or glass. A thermostatic bath (Figure 1) provides a good thermal stability, even for long-term experiments. The latter is thermo-regulated by two dedicated heaters.

All generated test gases run through rudimentary heat exchangers, which were immersed in the bath. Relative humidity could be precisely regulated within a large range. A dedicated mixing chamber (M in Figure 1) was connected to incoming sample gas and to vapour-saturated air provided by a humidifier. Regulation of each incoming flow allowed a relatively accurate and steady control of the final sample relative humidity. Both temperature and relative humidity were accurately monitored in each chamber by dedicated ozone-resistant sensors. Temperature was kept constant as much as possible, between 20°C and 25° C, with relative standard deviation below 1 % during testing sequence. Relative humidity was set to 30 %, with RSD below 1 % during each testing sequence. No particular flow restriction could be found in the set-up and it was therefore assumed that all the measurements took place at atmospheric pressure in the testing chambers. The atmospheric pressure was not monitored but it is assumed that pressure has little effect on the sensors.

A standard dilution system generated all the necessary samples by diluting traceable primary gas standards (NO and CO) with zero-air. The calibrator was equipped with a UV lamp-based O_3 generator and a photometer which enabled accurate O_3 production. NO_2 was generated by mixing O_3 and NO in a borosilicate glass chamber inside the calibrator (Gas Phase Titration). Testing gases were generated at different concentrations in a relatively large range, only limited by concentration level of reference gas cylinder and mass flow controller ranges.

All gas measurements were performed by CEN approved analysers. Table 8 gathers all the information regarding all used instrumentation. Gas analysers were connected at the output of the measurement chambers. They were regularly calibrated by connecting them directly to the gas calibrator. The test protocol consists of a multi-point calibration involving five different gas levels plus zero-air. Concentration step changes were performed at constant temperature and relative humidity.

Generation of one single gas at a time allowed separate calibration of each sensor. It also provided information about cross-sensitivity issues, since all platform micro-sensors were measuring simultaneously. Observed cross-sensitivity was reported with a simple scale including none (N), low (L) and high (H). Some data series showed cross-sensitivity.

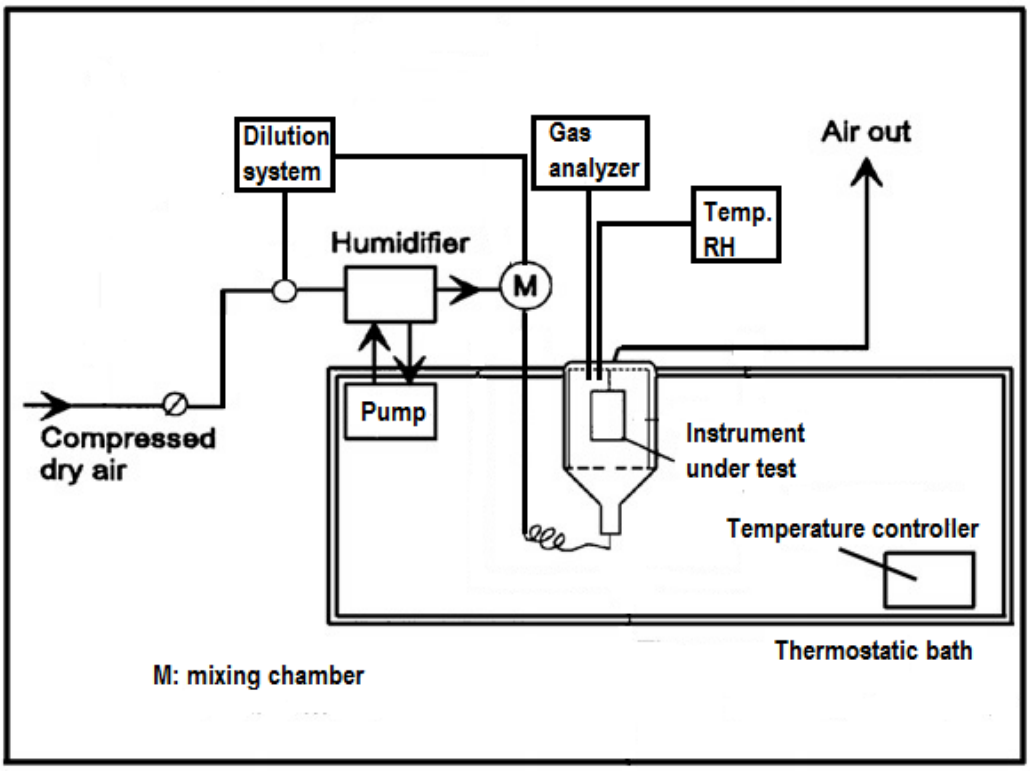

Figure 1. Set-up description

Table 8. Laboratory instrumentation

Instrument type	Instrument	Measurement Method	Detection limit / Accuracy
CO analyzer	Teledyne API 300E	Non-dispersive IR spectroscopy (EN14626)	40 ppb/
NO_x analyzer	Teledyne API 200A	Chemiluminescence (EN 14211)	0.4 ppb
O_3 analyzer	Teledyne API 400	UV photometry (EN14625)	0.4 ppb
SO_2 analyser	Teledyne API 100A	UV fluorescence (EN14212)	0.4 ppb
Zero Air Supply (For NO, NO_2, O_3, SO_2 and CO)	Custom-made	Filter, scrubber, activated and heated reactor	N.A.
Dynamic calibrator	Teledyne API 700	MFC (0 – 1000 sccm/0 - 50 sccm) Output (0 – 10,000 sccm)	N.A
Temperature sensor	Rotronic Hygroclip2-S	Pt100	N.A / 0.1% (@0° C)
RH sensor	Rotronic Hygroclip2-S	Hygromer	N.A. / 0.8% (@23° C)

Results

Table 9 shows the results obtained in the laboratory for the different platforms analysed. The laboratory results show that AQMesh unit 688150 have a linear behaviour, with good correlation for all tested gases ($r > 0.9$). The O_3 sensor suffers very low cross-sensitivity with NO_2 and the NO_2 shows no cross-sensitivity with O_3.

Results for NO show a good correlation ($r > 0.9$) between the units and the reference analyzer. Some NO peaks up to 66 ppb were generated erratically during O_3/NO_2 calibration sequences. There was no sign of correlation between these peaks and gas generation of other gases (NO_2, CO or O_3) which makes it difficult to draw conclusions regarding cross-sensitivity.

Results for NO_2 show there is a good correlation ($r > 0.9$) between the AQMesh and the reference analyzer. The NO_2 sensor reacted with a low peak (ca. 7 ppb) at the beginning of each O_3 calibration sequence, with O_3 set-point at 180 ppb. It also reacted to NO, but only at the beginning of first NO calibration sequence. The units showed no cross-sensitivity with O_3.

Results for CO showed a good correlation between the sensor and the reference analyzer ($r > 0.9$). It is important to note that CO gas generation for the low levels required using the lowest part of MFC measuring range from the calibrator. This range is not considered as a usable part of the range, as it has higher uncertainty in the measurements.

The laboratory tests indicated that good data quality was achievable with the current sensor technology, provided the sensors are tested under steady temperature and relative humidity conditions. All the sensor platforms chosen for the final deployment (AQMesh, Ateknea, Atmospheric sensors) showed excellent correlation with the reference instruments ($r^2 > 0.97$), with sensor sensitivities (gain; Table 10) between 0.7 and 1.22.

Only one major cross-sensitivity issue has been identified, a cross-sensitivity between the NO_2 and O_3 sensors. The latest NO_2 sensors delivered by Alphasense addressed this issue by developing advanced filtering solution, which seemed to offer an effective rejection of O_3. Yet, no modification was done for the O_3 sensor, which showed similar sensitivity to O_3 and NO_2. Accurate O_3 measurements required, therefore, algorithms involving outputs from both O_3 and NO_2 sensors (differential mode).

Lab tests done on the latest versions of all three chosen platforms showed that only AQMesh implemented such algorithms. The laboratory tests done with the AQMesh unit gave quite positive results. Ateknea and Atmospheric Sensor platforms apparently displayed raw outputs from these sensors. O_3 sensors from these platforms showed strong cross-sensitivity with NO_2 (see Table 9).

Table 9. Summary of all platforms, including linear fit when compared to reference measurements.

Platform	Data Average Time (seconds)	Species/ parameter	Coefficient of determination (r^2)	Gain	Intercept [ppb]	Observed cross-sensitivity between gas species)
AQMesh	900	CO	0.99	0.86	0.07	NO_2:N,O_3:N,NO:N
		NO	0.99	0.97	-1.13	NO_2:N,O_3:N,CO:N
		NO_2	0.99	1.22	-1.02	O_3:N,NO:N,CO:N
		O_3	0.99	1.16	-1.27	NO_2:L,CO:N,NO:N
Ateknea	60	NO_2	0.99	0.86	23.9	NO N, O_3:N
		NO	0.99	0.71	-21.5	NO_2:N, O_3:N
		O_3	0.96	0.70	-7.7	NO: N, NO_2:H
Atmospheric sensors	300	CO	0.99	0.77	34.93	NO:N,O_3:N,NO_2:N
		NO	0.99	0.82	8.38	CO:N,O_3:N,NO_2:N
		NO_2	0.99	1.03	33.55	NO:N,CO:N,O_3:H
		O_3	0.97	1.07	47.25	NO:N,CO:N,NO_2:N
Airbase	300	NO_2	n.a.	n.a	n.a	n.a
Dunavnet	n.a	NO_2	0.92	1.87	2859.8	
		O_3	0.91	-0.69	2758.4	
		NO	n.a	n.a	n.a	

Table 10. Repeatability of measurements

Platform	Data Average Time [seconds]	Species/ parameter	Mean measured value ±std dev. with 0-air [ppb]	Mean reference value ± std dev with 0-air [ppb]	Mean measured value ±std. dev.at 100 pbb span (*) [ppb]	Mean reference value ±std. dev.at 100ppb span [ppb]
Environmental Instruments AQMesh	900	CO	16.3±6	-21.9±9.7	1292±21.5	1385±16.2
		NO	n.a	0.4±0.4	88.5±1.5	94.1±0.9
		NO_2	n.a	0.7±0.3	126.4±3.5	103.9±0.7
		O_3	n.a	0.8±0.2	123.4±2.3	108.5±1.5
Ateknea LEO	10	NO	-15.3±10.8	0.4±0.3	49.0±8.7	94.3±0.6
		NO_2	24.7±3.1	0.3±0.2	117.9±3.3	107.7±0.4
		O_3	-6.8±4.1	0.5±0.5	57.5±3.4	86.1±0.6
Atmospheric sensors	300	CO	n.a	32.9±11.6	3940.5±20.0	4930.0±26.8
		NO	13.8±4.8	0.4±0.7	93.3±5.0	94.3±1.1
		NO_2	33.7±5.6	0.3±0.2	142.9±1.2	106.3±0.8
		O_3	41.5±17.1	0.6±0.2	136.8±4.1	84.9±1.2

(*): except for CO where 1300ppb was used as span value with AQMesh and 5000ppb with Atmospheric Sensor node

5 Sensor Evaluation Under field conditions

Static Units

Based on phase I results, we expected limited detection, sensor degradation in the outdoor environment and poor selectivity to the gaseous pollutant by both the MO and the electrochemical sensors. This motivated us to perform a more comprehensive testing of the sensors, to set criteria to characterize the nodes actual (field) capabilities, to suggest and test various sensor calibration options, and to understand what the technology can detect, measure, and used for by regulatory personnel, NGO, empowered citizens, and the scientific community. Specifically, setting various criteria for various applications allowed us to assess the sensors' performance for different tasks and applications.

The first task in phase II was to develop a comprehensive Sensor Evaluation Toolkit (SET) for evaluating and comparing the nodes performance and application. This work has been done using 25 nodes deployed in eight cities in Europe, as part of WP2 deployment within the CITI-SENSE project. All the nodes were collocated at AQM stations for three months, and their measurements were compared against those acquired by the AQM (Fishbain et al., 2016). While the SET requires a reference device to evaluate the sensor measurements, it does not make an assertion on the nature of this reference equipment. The evaluation involves a comparison of two concentration time-series: one acquired by the sensor and one obtained by the reference device. Without loss of generality, both time-series should be of equal length, i.e. consist of *K* measurements with the same measurement frequency. The SET consists of two common performance measures, RMSE and correlation, and four new measures: *presence* (represents the sensor reporting reliability), *source-analysis* (depicts how accurate a sensor is when it is used for a source identification), *match* (evaluates the sensor's accuracy when the measured concentrations are transformed into generalized coarse scales), and *Lower Frequencies Energy Content (LFE)* (measures the nodes' ability to capture the temporal variability of the observed pollutant). All the measures are then combined to an Integrated Performance sensor Index (IPI).

Table 11 depicts the average values of the measured environmental parameters, showing that the nodes' meteorological measurements are more accurate than the pollutant concentrations. The atmospheric pressure, temperature and relative humidity (RH) sensors have, on average, an IPI of 0.975, 0.875 and 0.851, respectively. Among the pollutants, the NO sensors had the highest IPI, with an average of 0.705. O_3, CO and NO_2 obtained IPIs of 0.664, 0.609 and 0.578, respectively. The utilization of the SET for evaluating WDSN node performance is well demonstrated in Table 11. Sensor 143, which had lower IPI values for all measured environmental parameters, may have experienced a systematic error due to incorrect placement of the sensor or malfunction of hardware. Sensor GAP 4 presented low IPI for RH. The average RH value that this sensor reported (106.4%) clearly suggests that the sensor is faulty or overly-offset for this parameter. Sensor 118 presented low IPI for CO and NO while their average concentrations were much higher than those measured by the AQM and other collocated nodes. These measurements were removed from further analysis.

Table 11. Environmentally sensed indicators - mean values (M) and Integrated Performance Index (IPI) for Air Pressure (AP), Temperature (Temp), Relative Humidity (RH), nitrogen oxide (NO), nitrogen dioxide (NO2), ozone (O3), and carbon monoxide (CO).

Unit	Location	AQM Temp	AP		MSU Temp		RH		NO		NO_2		O_3		CO	
			M	IPI	M	IPI	M	IPI	M	IPI	mean	IPI	M	IPI	M	IPI
GAP1	Gal-la Placídia Barcelona Spain	23.62	1007	0.949	24.5	0.887	61.6	0.863	6.2	0.656	13.6	0.464	133.8	0.687	162.9	0.587
GAP2		23.62	1008	0.952	24.5	0.892	62.0	0.864	0.1	0.412	0.8	0.455	178.6	0.669	177.0	0.572
GAP3		23.62	1008	0.950	24.5	0.894	60.8	0.853	1.0	0.557	9.4	0.497	65.4	0.699	137.9	0.584
GAP4		23.62	1008	0.944	24.3	0.897	106.4	0.382	16.2	0.667	9.6	0.503	144.8	0.675	159.0	0.569
GAP5		23.62	1009	0.957	24.5	0.901	68.7	0.543	1.9	0.638	1.8	0.481	153.8	0.674	148.3	0.576
116	St Leonards, Edinburgh, Scotland	-- [13]	-- [13]	-- [13]	-- [13]	-- [13]	-- [13]	-- [13]	7.8	0.513	11.7	0.409	51.2	0.649	58.8	0.524
118									138.0	0.501	8.5	0.394	66.9	0.604	433.3	0.451
120									9.7	0.514	9.9	0.413	42.5	0.627	54.1	0.482
135	Neve Shaannan, Haifa, Israel	12.95	-- [13]	-- [13]	14.7	0.717	57.5	0.860	3.2	0.513	2.7	0.621	71.2	0.663	103.2	0.562
136		12.95	-- [13]	-- [13]	14.4	0.689	57.0	0.842	3.3	0.508	5.0	0.640	44.8	0.697	94.4	0.552
130	Igud, Haifa, Israel	12.97	-- [13]	-- [13]	13.6	0.712	57.3	0.829	7.2	0.620	-- [13]	-- [13]	52.3	0.641	-- [13]	-- [13]
134		13.65	-- [13]	-- [13]	14.9	0.705	58.1	0.802	5.9	0.633	-- [13]	-- [13]	41.9	0.633	-- [13]	-- [13]
125	Ljubljana, Slovenia	12.46	979	0.989	13.7	0.935	64.9	0.947	-- [13]	-- [13]	21	0.55	78.4	0.711	166.4	0.769
128		12.46	978	0.940	13.8	0.926	64.8	0.945	-- [13]	-- [13]	3800	0.46	105.8	0.687	175.0	0.681
131		12.46	980	0.934	14.1	0.908	63.6	0.937	-- [13]	-- [13]	6	0.54	96.9	0.719	179.8	0.663
124	Kirkeveien, Oslo, Norway	6.80	1009	0.988	7.9	0.931	84.2	0.889	27.2	0.921	15.5	0.685	-- [13]	-- [13]	101.2	0.710
144		6.80	1007	0.990	7.9	0.945	83.1	0.895	30.5	0.869	16.9	0.637	-- [13]	-- [13]	95.6	0.697
145		6.80	1008	0.989	7.8	0.937	84.5	0.893	23.0	0.860	16.5	0.712	-- [13]	-- [13]	98.8	0.704
146		6.80	1008	0.988	7.9	0.937	84.2	0.896	37.3	0.899	13.7	0.697	-- [13]	-- [13]	102.1	0.682
147		6.80	1008	0.989	7.9	0.945	83.3	0.892	25.9	0.876	14.4	0.565	-- [13]	-- [13]	94.5	0.592
124		7.26	1006	0.976	9.1	0.923	65.9	0.923	16.8	0.859	9.2	0.583	-- [13]	-- [13]	-- [13]	-- [13]
144		7.26	1004	0.993	8.8	0.933	66.9	0.931	16.8	0.871	12.2	0.651	-- [13]	-- [13]	-- [13]	-- [13]
145		7.26	1004	0.992	8.7	0.937	67.0	0.930	11.9	0.795	16.5	0.692	-- [13]	-- [13]	-- [13]	-- [13]
146	Hjortnes, Oslo, Norway	7.26	1005	0.978	9.1	0.924	66.2	0.923	9.8	0.732	12.6	0.647	-- [13]	-- [13]	-- [13]	-- [13]
147		7.26	1005	0.991	8.8	0.945	66.4	0.934	16.4	0.856	9.3	0.659	-- [13]	-- [13]	-- [13]	-- [13]
124		17.80	1011	0.983	20.4	0.911	63.0	0.907	15.4	0.842	17.7	0.654	-- [13]	-- [13]	-- [13]	-- [13]
144		17.80	1009	0.991	20.5	0.905	62.8	0.905	15.5	0.843	22.2	0.644	-- [13]	-- [13]	-- [13]	-- [13]
145		17.80	1010	0.989	20.4	0.918	63.7	0.911	5.9	0.760	26.9	0.700	-- [13]	-- [13]	-- [13]	-- [13]
146		17.80	1010	0.986	20.5	0.917	63.1	0.910	22.5	0.803	18.7	0.635	-- [13]	-- [13]	-- [13]	-- [13]
147		17.80	1010	0.988	20.6	0.920	61.9	0.912	12.7	0.828	15.6	0.634	-- [13]	-- [13]	-- [13]	-- [13]
611	Ostrava, Czech Rep.	1.06	992	0.975	4.6	0.901	80.5	0.911	-- [13]	-- [13]	-- [13]	-- [13]	30.5	0.736	-- [13]	-- [13]
612		1.06	991	0.971	4.6	0.896	80.8	0.895	-- [13]	-- [13]	-- [13]	-- [13]	26.3	0.773	-- [13]	-- [13]
221	Belgrade, Serbia	5.78	1008	0.685	5.7	0.885	82.8	0.810	69.7	0.794	27.5	0.591	35.8	0.585	519.8	0.691
222		5.78	1008	0.685	5.7	0.874	81.4	0.815	81.8	0.793	14.3	0.554	60.9	0.537	537.6	0.692
143	Vienna	5.08			15.1	0.473	62.4	0.402	13.2	0.387	5.5	0.348	126.0	0.402	-- [13]	-- [13]
Average IPI				0.953		0.876		0.848		0.711		0.577		0.653		0.617

[13] This specific environmental variable was not measured by the AQM at the colocation time period.

The richness of the IPI is demonstrated in Table 12 through a breakdown of the IPI into its components for two sensors: NO sensor of node 118 and Temperature sensor of node 130. The IPI components are the Mean (M), Match score, RMSE, Pearson (ρ), Kendall (τ) and Spearman (S) correlation coefficients, Source-analysis score, Presence (Pres) and Lower Frequencies Energy (LFE) content. For both sensors, the LFE is high, suggesting that the changes in the observed signal are slower than the sampling rate, hence the temporal patterns of these phenomena can be reliably reconstructed. Node 118 NO sensor measured extremely low correlations, while its match score is high. Thus, while this sensor would be ranked poorly using traditional evaluation tools (correlation and RMSE), it could be useful for many applications, such as citizen science and relative exposure estimation. The Temp sensor of node 130 also demonstrated interesting behaviour in the study period, presenting a reasonable Match score and correlation coefficients but very low RMSE. This suggests that while the sensor does not measure the true ambient temperature (i.e. had considerable bias) it did follow its variation (i.e. showed good

correlations). Therefore, a careful inspection of the different IPI components can provide a better understanding of the sensor performance and suitability for different applications.

Table 12. IPI breakdown: Mean ambient level (M), Match score, Root Mean Squared Error (RMSE), Pearson ρ correlation coefficient, Kendall τ correlation coefficient, Spearman (S) correlation coefficient, Source analysis, Presence (Pres), Low Frequencies Energy (LFE) content, and the integrated Air Quality Index (IPI).

Sensor	M	Match	RMSE	ρ	τ	S	Source	Pres	LFE	IPI
118 (NO)	129.9	0.920	0.24	0.063	0.068	0.090	N/A	0.732	0.976	0.519
130 (T)	13.63	0.462	0.003	0.679	0.538	0.712	N/A	1	0.997	0.712

Effects of meteorological conditions on the sensor measurements

Ambient temperature has been pointed-out as a major factor that could affect the sensor performance (Moltchanov et al., 2015; Lerner et al., 2015; Mead et al., 2013; Williams et al., 2013). However, the integrated average IPI of the 25 nodes did not reveal any apparent trends with respect to the average AQM temperature measurements (Table 11). While this may suggest that the nodes managed to compensate for any "direct" temperature impact on the measurements, the integrated index may also hide effects of the meteorological conditions on specific performance measures. In fact, one of the main challenges when using electro-chemical sensors is that they are reported to suffer from interference with the temperature and the relative humidity (Aleixandre and Gerboles, 2012; Mead et al., 2013). Only generic data that described the relationships between the sensor current response, the temperature and the relative humidity were available for us from the sensor manufacturer (Alphasense, UK). The AQMesh platform manufacturer implemented some correction factors for these effects. Yet, due to huge variability of the meteorological and climatological conditions among the project case-study cities, we examined how the bias (the difference between concentrations measured by the AQMesh node and the AQM reference equipment) varied with the temperature and the relative humidity. The nodes' performance varied: some showed no significant bias, some showed increasing bias as the temperature increased and some showed bias at specific temperature ranges. This indicated that the adjustments implemented by the AQMesh platform manufacturer worked only for some nodes, and that there is considerable variability among nodes – even from the same batch (Castell et al., 2016). In general, we found that the response of each sensor is unique, and that it is therefore necessary to examine each sensor node individually before deploying it in the field. In particular, the calibrations and correction factors supplied by the sensor and/or platform manufacturers were insufficient for correcting the measurements under real-world conditions, where large temperature and relative humidity variations are encountered (Castell et al., 2016). Moreover, further examination confirmed the advantage of applying post-processing methods, such as regressions, neural network and machine learning procedures, to correct for the impact of environmental conditions on the sensor readings (Sun et al., 2016; Spinelle et al., 2015). This, however, cannot be done in real-time and cannot improve the measurement stream from the sensor nodes, which in the CITI-SENSE project was planned to be queried in quasi-real time and fed to an app that can be used in "real-time" by interested stakeholders.

It further seems that apart from a direct effect of the temperature on the sensor measurements, the ambient levels of the pollutants also affected the measurement, with the sensors performing better at higher pollutant levels. Since higher pollutant levels are often observed in the winter, due to both higher emissions as a result of biomass burning in relation to space heating as well as temperature inversions and unfavourable dispersion/mixing meteorological conditions (Seinfeld and Pandis, 2016), it seems that previously reported temperature effects on the sensors' measurements could represent

also an "indirect" effect, resulted by the sensors' high detection limits compared to common ambient concentrations in urban areas. Namely, the seasonality of ambient concentrations, which is normally correlated with the ambient temperature, may be due to many factors, including planetary boundary layer height, solar radiation, wind patterns, temperature related emissions, etc., for which the temperature is a confounder. Indeed, Figure 2 depicts that the lower the ambient pollutant level, the lower the IPI and the higher its variance (i.e. the sensors have lower reliability at lower ambient pollutant levels). A similar behavior was observed by Lerner et al. (2015) and by Moltchanov et al. (2015). Hence, WSDN nodes seem to be more suitable for measurement in locations where the pollutant concentrations are expected to be high.

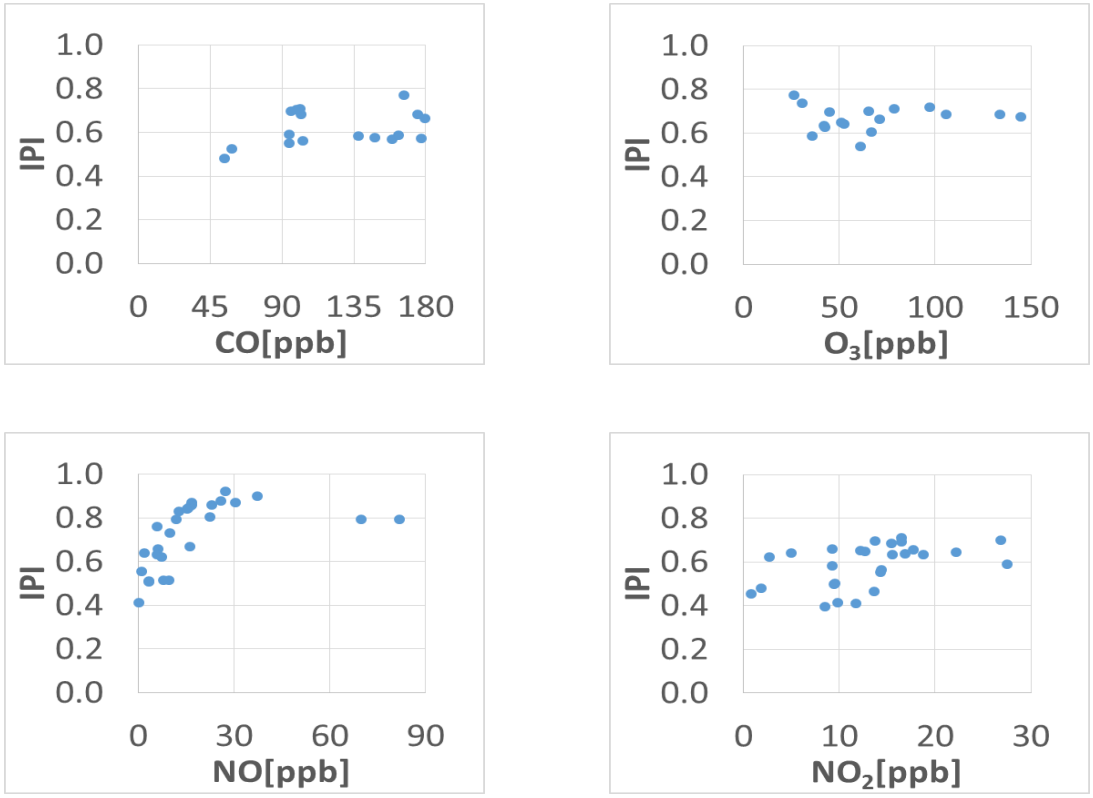

Figure 2. Effect of the pollutant average levels on the sensor IPI.

The aforementioned behaviour is better observed when the IPI is computed based on daily time series rather than when using the entire campaign time series. For example, Figure 3 depicts the daily IPI for NO_2 and NO from measurements obtained in Kirkeveien, Oslo, by sensor nodes 124, 144, 145, 146 and 147. It is evident that the variability of the IPI decreases as the pollutant concentrations increase. A reasonable threshold for the sensors' reliable measurement of NO2 and NO seem to be ambient concentrations of 30 ppb.

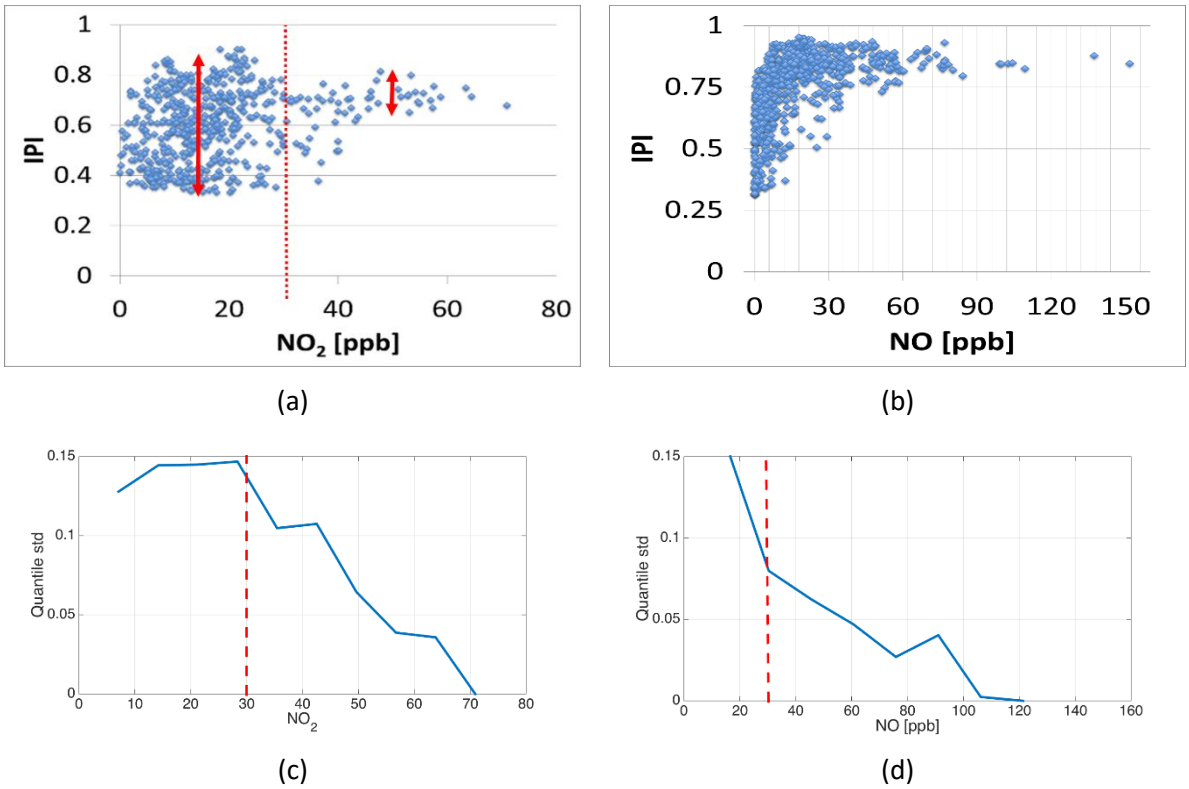

Figure 3. Daily IPI score as a function of NO_2 (a) and NO (b) records from Kirkeveien, Oslo. The standard deviation of the IPI for each decile of the pollution concentration are presented in (c) and (d) for NO2 and NO, respectively.

Figure 4 demonstrates how the IPI can be used for comparing between sensors and microenvironments, with a very clear effect of the ambient levels on the sensors' performance. The bimodal distribution corresponds to IPI scores above and below 30 ppb.

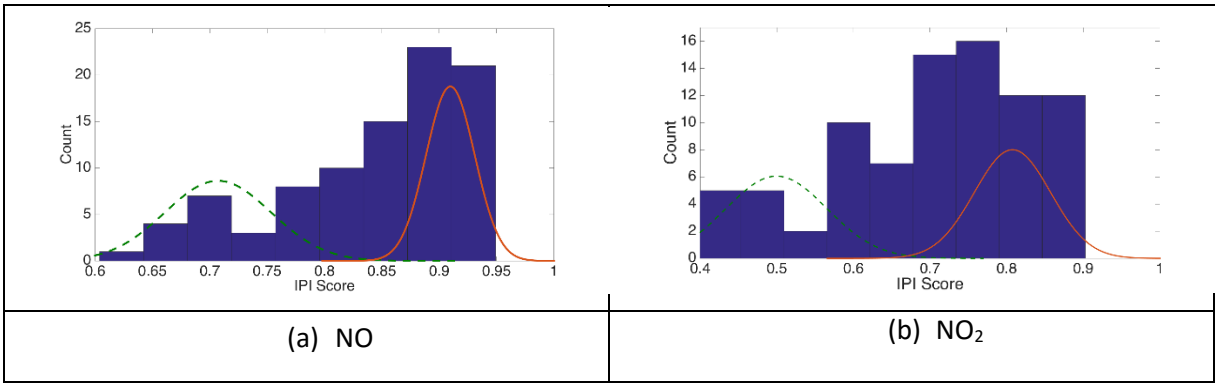

Figure 4. Distribution of the daily IPI scores for NO (a) and NO2 (b) measured at Kirkeveien, Oslo.

The SET was applied also for PM data measured by four nodes in Haifa, Israel. The four sensors included two calibrated DC1700 Dylos optical particle counters (OPCs), which served as reference measurements, and two optical counters that were integrated into the AQMesh nodes (ver. 3.5). Fine PM mass measurement from the collocated AQM was also recorded. The different physical units of the measurements affect only the RMSE measure whereas the other SET measures can be still used. In general, our results suggest that the (converted) mass measurements of the AQMesh nodes are better than the performance of the gaseous pollutant sensors when compared to AQM data. However, the

number concentration measurements of the Dylos seem to be even better than the AQMesh mass PM data. Hence, we recommend that in the future particle number concentration rather than mass-based PM records will be included in WDSN nodes, since, as shown, the sensor are anyhow not suitable for serving for regulatory purposes (see also below). Information on personal exposure to particle number concentration may be more useful for citizen empowerment than PM mass measurement, since it is expected to capture more intra-urban variability that result from anthropogenic sources and varying land use.

Land Use Effects

To evaluate the sensor performance in different urban microenvironments, the nodes were collocated between 1st July - 22nd September, 2015, at three reference stations: Kirkeveien and Manglerud (near busy roads) and Åkebergveien (a calm street), Oslo, Norway. For NO_2, poor correlations (<0.7) were obtained in all the three locations. For NO, the correlations were in general acceptable in all the three stations although they were lower at Åkebergveien AQM station (0.5-0.8) than in the two traffic-affected AQM stations (0.8-0.9) (Castell et al., 2016). This clearly reflects the lower NO_x concentrations at urban background AQM stations compared to stations close to dense traffic, and is in line with our previous findings (e.g. Figures 2-3). Oslo findings also agree with Belgrade results, where similar study design was practiced by collocating AQMesh units in a traffic type AQM station (Zeleno Brdo, 21st April – 7th July, 2015) and an urban background AQM station (Stari Grad, 14th July – 16th October, 2015) in Belgrade for 3 months, followed by relocating the units next to a street with low/medium traffic. Like in Oslo, the 25 nodes demonstrated lower correlations when the NO_2 concentrations were low. The Belgrade team also collocated and tested 12 Atmospheric Instruments Model 510 nodes in both the urban background AQM site and the traffic related AQM site. Again, while the Pearson correlation coefficients were very high (>0.7) for all the measured pollutants (CO, NO_2, O_3) low correlations with reference AQM records were obtained.

For particulate matter, better results were obtained at a calm street microenvironment, with correlations of 0.7-0.8 for PM_{10} and 0.8-0.9 for $PM_{2.5}$. At the traffic impacted microenvironment r<0.4 were obtained for both PM fractions. As explained previously, the AQMesh node estimates PM mass concentrations based on OPC sensors that measure the number concentrations. The conversion factors that the AQMesh platform manufacturer used to obtain PM mass concentrations seem to suit better background sites. Our result that the AQMesh nodes suit better PM measurement away from busy roads is in fact opposite to our results regarding the gaseous sensors, where we showed that the sensors perform better at microenvironments that are characterized by higher pollutant levels. These results have two significant implications. First, ultrafine particles are freshly emitted or formed in traffic-busy microenvironments. Since their composition differ considerably from particles found in background sites, due to aging and restructuring (Broday and Rosenzweig, 2011), they are expected to have different toxicity and to inflict distinct adverse health effects. It seems that in urban areas exposure to that PM fraction will not be assessed correctly with the current PM measurements of the AQMesh nodes. Moreover, it seems that the deployment of multiple sensor nodes may involve contradicting aspects. Namely, if gaseous pollutants are the target pollutants than the nodes should be deployed near traffic arteries, where pollutant levels are higher and so is the sensor performance. However, if PM concentrations are the goal then the nodes should be deployed away from busy traffic arteries, since PM mass is “blind” for the ultrafine particles and the sensor’s “converted” mass readings are better away from bust roads. Clearly, if PM number concentrations will be reported these considerations will change and the deployment scheme of gaseous pollutant sensors and of particle number concentration sensors are expected to align.

Sensor Calibration in the Field

Various alternatives for the sensor field calibration were explored within the CITI-SENSE project. The simplest approach is termed collocation and refers to measurements performed in parallel by a

reference (and periodically calibrated) device, normally an AQM station analyser, and by several WDSN nodes that are collocated at the AQM site. We observed that the intercept and offset obtained in the laboratory were not valid in the field. For example, CO sensor had an offset of 166 ppb in the field compared to an offset of only 0.07ppb in the laboratory tests (Castell et al., 2016). Moreover, the field calibration was also dependent on where the sensor was located. Hence, the intercept and gradient varied when the sensor was deployed in an urban traffic location or in a background location (Castell et al., 2016). Overall, when deployed in the field the sensor characteristics were not as good as when tested in the laboratory, and their sensitivity to varying ambient temperatures, relative humidity and air matrix concentrations was higher. This highlights the importance of calibrating the nodes in an environment similar to the one in which they would be deployed, or better to perform in-situ calibration at the deployment sites. Different methods for field calibration have been examined.

Field calibration of metal oxide O_3 sensors mounted on the AirBase platform was examined in the Haifa case study. The individual nodes' gain and bias coefficients were found to change significantly over time (Figure 5). The temporal change of the regression coefficients was attributed to aging of the sensors (resulting in alterations in the gain; Williams et al., 2013) and to episodic events such as rain and dust storms that cause dirt to accumulate on the sensors (Figs. 5c,d). The sensor-specific temporal variation of the calibration parameters resulted in a non-linear inter-nodal (i.e. relative) divergence of the readings and called for a frequent field calibration of the nodes. Since frequent collocation of numerous WDSN nodes at an AQM station is clearly impractical, a different method for field calibration was sought, as presented below.

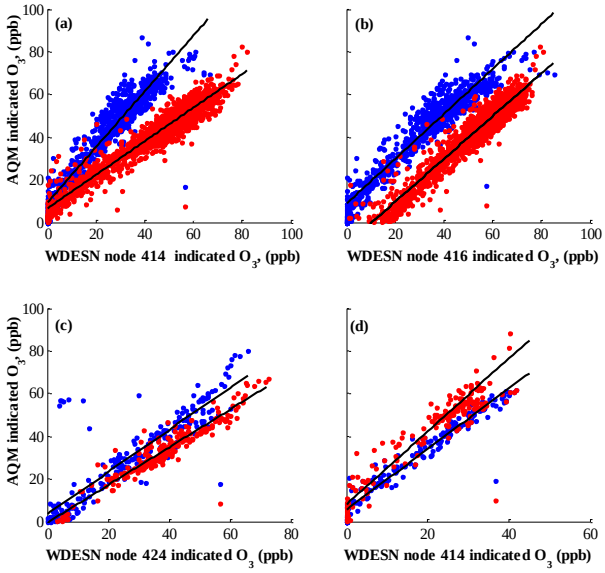

Figure 5. Comparison of WDSN ozone measurements with AQM reference measurements performed at different periods during 2013 (30 minutes averages), Haifa. (a) Node 414, (b) node 416, (c) node 424 before (blue) and after (red) a rainy period, and (d) node 414 before (blue) and after (red) a dust event.

Relative air pollution indication

The emergence of low-cost sensors has shifted the paradigm of who can monitor air pollution. Historically, air pollution was monitored by governments and scientific institutions. Nowadays, many small companies offer air pollution monitors to citizens at affordable prices. However, there is a lack of testing to ensure adequate sensor performance prior to marketing of such instruments. We evaluated if the AQMesh platform V3.5 meet the criteria defined in the Air Quality Directive

2008/50/EC (AQD; EU, 2008) and can serve for regulatory purposes. Our results showed that for the regulatory pollutants (NO2, O3, PM10 and PM2.5) the uncertainty does not meet the data quality objectives (Castell et al., 2016). However, it t can be argued that for most citizen applications the data quality does not need to reach the same quality standards as necessary for air quality management by authorities or for research.

The SET match score offers information whether the sensor is able to capture a coarser indication of air pollution, i.e. if the air pollution is very poor, poor, good or very good. When computing the SET match score for the AQMesh platform v3.5, NO and PM_{10} showed very good potential to report consistent relative air quality values, with an average match score close of 0.8 and 0.9, respectively. For NO_2, CO, O_3 and $PM_{2.5}$ the match score was <0.5, indicating that even the relative agreement between the sensor platform and the station (e.g. high vs. low with respect to neighbouring measurements that each sensor/technology measures) was not good (Castell et al., 2016). This however does not mean that the current sensors cannot be used for applications that even relative measurements are of less importance but that e.g. want to raise the awareness to air pollution and empower citizens to be aware and reduce their personal exposure as much as they can. Such application may include citizen science, hands-on filed-lab science, educational purposes, etc. As an example, Figure 6 depicts the capability of WDSN nodes to perceive the pollutants' spatial variability at the neighbourhood scale. In particular, the three sites were Moltchanov at al. (2015) deployed the (paired) WDSN nodes were located only ~100–150 m apart, within a residential neighbourhood in Haifa, Israel. The sites were readily distinguishable based on the WDSN nodes measurements.

Some of the WDSN sensors (e.g, NO and PM10) are shown to be capable of reproducing the time variation measured at the reference station. Thus, even if the data uncertainty is too high for use for legislative purposes, some sensors can still offer useful information to concerned citizens. It is important to note that with future progress and reproducibility of WDSN sensor technology, it is possible that our results will be relevant for more pollutants and environmental conditions that the current state-of-the-science in distributed sensing technology enables.

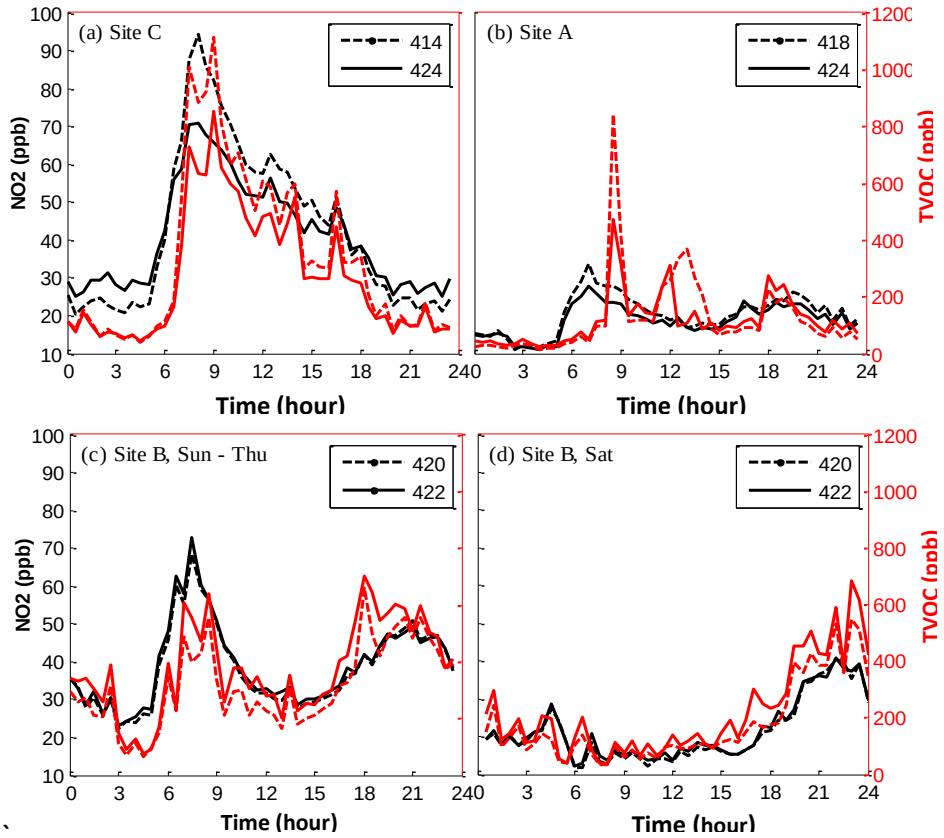

Figure 6. Daily patterns of 30 min average NO_2 (black) and TVOC (red) concentrations at (a) site C during weekdays (Sunday–Thursday) on Period II of the measurements, (b) site A during weekdays on Period III of the measurements (to demonstrate the responsiveness of the TVOC sensor of node 424 to its new microenvironment, as sensor nodes were rotated among the deployment sites in this study), (c) site B during weekdays on Period II of the measurements, and (d) site B during Saturdays on Period II of the measurements. The solid and dashed lines correspond to collocated nodes in the field (i.e. not at an AQM station).

Alternative field calibration approaches

In a collocation field calibration, the nodes are placed adjacent to AQM stations and their measurements are compared against those acquired by the AQM, whose equipment is assumed to provide the reference readings. The SET was shown to be able to analyze such sensor data against the reference data, and to evaluate the nodes (before and after calibration) in multiple and rich ways. However, since the SET does not make any assertion on the nature of the reference measurement, without loss of generality any two time-series can be compared against one another as long as they have of equal length. Thus, for example, we used the SET to evaluate the AQMesh total particle count sensor (before the measurement is converted to PM mass measurement). Fot this, we used data collected in Barcelona in spring-summer, 2016. In general, the AQMesh OPC sesnor was found to perform better than the cheapest off-the-shelf particle sensor nodes (e.g. TZOA) in all parameters. Moreover, studying the sampling frequency, it is clear that with higher sampling frequency (e.g. 1 min) the data time series is much richer than with a lower sampling frequency (e.g. 15 min or 60 min). The richer time series seems to affect the Match Score, which seems to be linked to the sampling resolution and the richness of the data it provides. Namely, there are fewer cases where the averaging of the measurements over the extended sampling period introduced errors that changed the relative rank of the measurement relative to neighbouring time-series data-points. In fact, this suggests that using 1 min resolution when reporting the CAQI (Community Air Quality Index) for particle number

concentrations (and more precisely, sub-micron particles) might be more useful for non-scientists and non-regulators, e.g. for concerned citizens, educational purposes, and the general public. However, for applications that required accurate absolute levels some averaging (e.g. 5 min or 15 min) is expected to reduce the measurement noise (instrumental as well as due to extremely fast micro-meteorological condition). As mentioned above, in general and even after the particle counts are transformed into PM mass concentrations, the AQMesh sensor seem to be more reliable than its sensors for the gaseous pollutants. In particular, on average it suffers less deterioration over time and hence its calibration is expected to last for longer times, which facilitates node calibration and should save maintenance and WDSN management costs.

The first field (i.e. not while collocated but rather while deployed in the field) calibration procedure we examined was based on calibration of the O_3 sensors against a nearby AQM station data. Data used for deriving the calibration coefficients were from 01:00-04:00 am, since during this time period urban anthropogenic (i.e. local) emissions of O_3 precursors (NO_2 and TVOC) are negligible due to the cease of traffic and the absence of solar radiation. Hence, ozone production (due to photochemical reactions) and depletion (due to titration with fresh NO) were expected to be insignificant, and O_3 concentrations tend to be relatively homogeneous and to reveal insignificant spatial variation on the urban residential neighborhood scale. Thus, we presumed that between 01:00-04:00 am the WDSN nodes in the Neve Shaanan neighborhood, Haifa, and the AQM station (deployed ~600-800 m away) reported similar concentrations. A sensor-specific linear regression was developed (based on 30 min averages, to fit the temporal resolution of the AQM data) for different deployment time periods and the regression coefficients were used for algorithmic adjustment of the sensor O_3 readings in the corresponding period, thus circumventing the effects of aging and general sensor degradation. At the evaluation stage (collocation with the AQM), this procedure was found to reduce the average mean absolute deviation between the collocated WDSN O_3 sensors from 13.3 (3.8-31.0) ppb (uncalibrated measuremnts) to 1.3 (0.6-3.1) ppb (after calibration based on data from the field deployment period). Daily O_3 patterns at the three sites during weekdays (Sunday–Thursday) and weekends (Saturday) are depicted before and after the calibration adjustments (Figure 7). The O_3 patterns (Figs. 7b,e) indicated that the in-situ night-time calibration procedure can overcome the disparity among ozone sensor measurements and bring them to a common ground (at night) while still revealing spatial variability during the day (resulting from variability of traffic related emissions across the neighborhood).

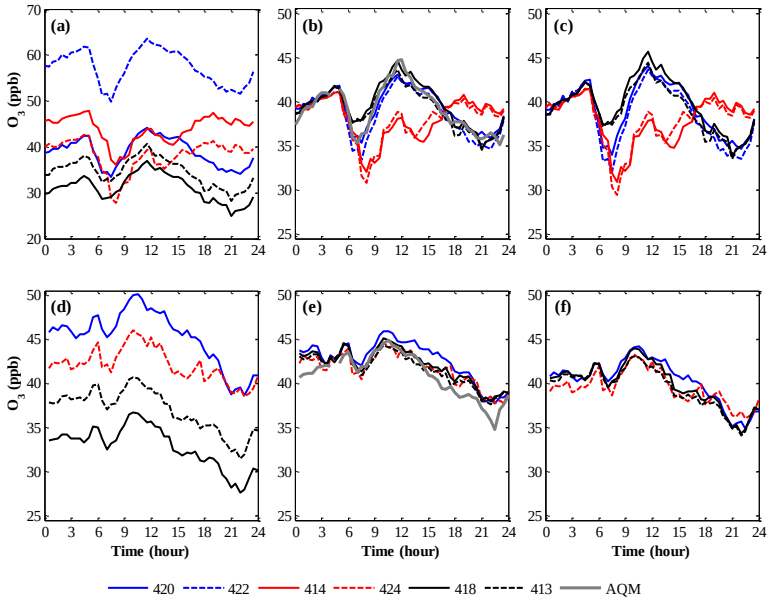

Figure 7. Daily patterns of 30 min. average O_3 concentrations during weekdays (Sunday–Thursday; upper row) and Saturdays (lower row) before calibration (a and d), after calibration based on AQM data from 1:00-4:00 am (b and e), and after calibration based on the mean 1:00-4:00 am value of all the WDSN nodes in the neighborhood (c and f). The O_3 sensors of nodes 414 and 422 stopped working on day 38 of the deployment, therefore the patterns shown in plates a-c are based only on data from days 28-38 (with calibration performed using data collected at the previous 27 days).

Most neighborhoods within any city do not have an AQM station within their boundaries, whose data can be used as a reference value for such a calibration procedure. In such cases, rather than using AQM data we examined the use of the 01:00-04:00 am mean value of all the nodes within the neighborhood. Whereas this procedure cannot calibrate the sensors against true reference values, it is shown that it does bring all the sensors to the same neighborhood-scale baseline, enabling to reveal the relative spatial variability of O_3 levels during the day (Figs. 7c,f) and reducing the mean absolute deviations among collocated sensors (0.7-3.7 ppb).

Moltchanov et al. (2015) derived also a theoretical calculation, assuming linear relationships between the sensor' readings and the reference measuremnts, for the calibration of individual sensors to the mean reading of all the sensor in its neighborhood (with the "neighborhood polygon" pre-set in advance based on land use/cover parameters and/or other factors). This calibration approach, and the theoretical derivation behind it, were designd specifically for pollutants for which the assumption of pollutant concentration homogeneity during the night hours is valid. Such an assumption fits more accurately secondary pollutants (e.g. pollutants formed in the atmosphere from precurssor emissions rather than directly emitted to the atmosphere), such as ozone, or pollutants whose major contribution is due to long range transport, such as PM. The theoretical derivation prooved that the relative ranking of the sensor readings (i.e. the SET Matched Score) are not disrupted. Consequently, as long as the "local scale" homogeneity assumption is valid, night time calibration to the mean value of all the O_3 nodes within the neighborhood has been shown to provide a useful method for qualitative determination of locations with higher (lower) pollutant concentrations. As for quantitative interpretation of the sensor measurements, using this calibration approach generally does not preserve the ratio or the difference between the actual concentrations at the different WDSN measuremnt locations. It is noteworthy that measurements in Haifa suggested that the differences in ozone concentrations measured at different locations by the WDSN nodes following calibration to the mean nighttime neighborhood AQM data correspond closely to the spatial concentration differences

infered from the calibrated sensor measuremnt, following calibration to the mean nighttime neighborhood sensor readings (Moltchanov et al., 2015). Yet, further research is clearly required to assess the propagation of errors generated by the two proposed field calibration procedures.

The regression coefficients of the two field calibration procedures discussed above (i.e. against the AQM late night mean and against the sensors late night mean) were demonstrated in Haifa based on all the data points between 01:00-04:00 am of the relevant phase I study period. However, it is possible to apply these procedures also in a predictive mode, i.e. with the calibration coefficients for each day calculated based on the 01:00-04:00 data from the same day or from previous days. Since at the time this study was performed the WDSN data available for us did not cover a sufficiently long period, only preliminary results that demonstrate the concept, using 5 min averaged O_3 AQM data. Figure 8 depicts changes in the regression slope, intercept and R^2 as a function of the number of nights (i.e. data points) used. As seen, whereas data from one night is insufficient for obtaining reliable regression parameters they tend to stabilize using data from 2–4 nights (Figs. 8b-d). Using data from longer periods seems to introduce disturbances and deteriorate the results, in accordance with Yuval and Broday (2010), where ozone concentrations from periods longer than 4 days were shown to be uncorrelated (Figure 9). Therefore, calibration coefficients for each day were calculated based on AQM data from 1:00-4:00 am of the three preceding days. This rolling forwards field calibration procedure reduced the average mean absolute deviation between collocated WDSN O_3 measurements from 3.7-18.7 ppb to 0.5-1.1 ppb, and enabled revealing the spatial variability of daily O_3 concentrations (Figure 8a).

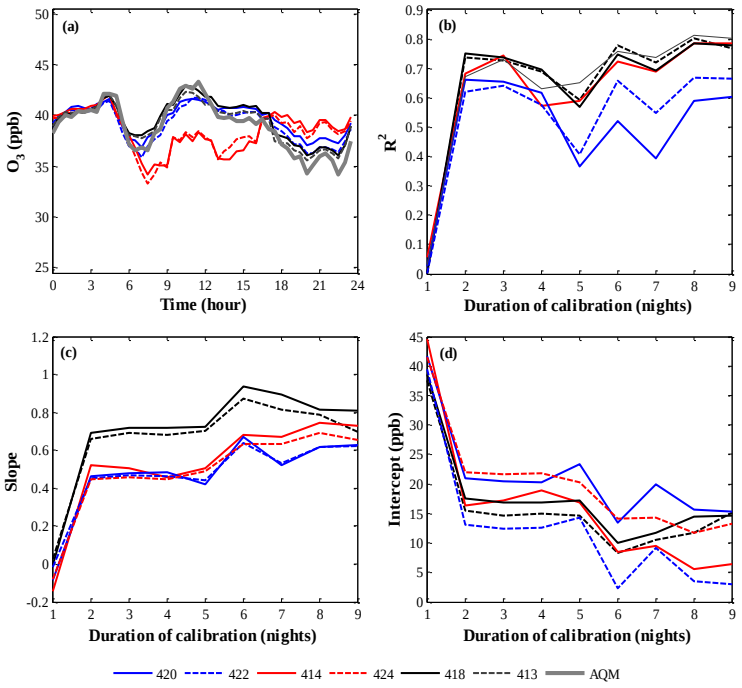

Figure 8. Daily patterns of 30 min average O_3 concentrations during weekdays (Sunday–Thursday) after daily calibration against AQM data from 1:00-4:00 am of the three previous days (a), and variation of the oefficient of determination of the regression, R^2, (b), the regression slope (c) and intercept (d) with the calibration duration.

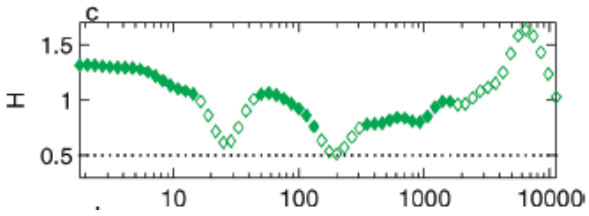

Figure 9. Spectrum of values of the Hurst parameter, H, as a function of the temporal scale for the O_3 records from the AQM station in Nave Shaanan, Haifa. The x axis represents time points (30 min). The empty markers denote H values not considered suitable for predictive estimation. The dotted line at H=0.5 denotes complete randomness (unpredictability). Figure adopted from Yuval and Broday (2010).

It is noteworthy that the concept behind the proposed field-calibration procedures can be applied to other air pollutants as long as they exhibit negligible spatial variation for a sufficiently long period, provided that the true concentrations are above the sensors' detection limit. Unfortunately, this criterion did not hold for NO_2 (which is neither purely primary nor "classical" secondary pollutant) in Haifa (as well as in other locations). This track of research was halted in late stages of the CitiSence project, since the project consortia as a whole moved (in phase II) to use other sensor platforms (uniform at all cities) for which the O_3 measurement were not as good, and since calibration of other sensors (of primary pollutants, for which the assumption of Moltchanov et al. (2015) does not hold) were needed. This will be described briefly below.

Yet, still another calibration approach stems its strength from the concept of group-decision-making in environmental sensing, and offers a valuable tool for aggregation of WDSN data. The suggested methodology presents a new, robust and efficient method for aggregating measurements acquired by an uncalibrated, inexpensive and error-prone WDESN, and producing accurate estimates of the observed environmental variable's true levels. Given a set of collocated MSUs, the scheme is applied where each measurement (defined by time and location) is considered as a referee evaluation. These time series can be incomplete as sensors might become faulty or shift locations. Based on a set of collocated measurements (in time and space) a consensus measurement is derived.

The methods has been applied to a wide set of pollutants measurements (i.e., ozone, nitrogen oxide, nitrogen dioxide and carbon monoxide) acquired by all available MSU technologies (metal oxide and electrochemical). When compared to a standard regulatory Air Quality Monitoring (AQM) station, the suggested methodology has shown markedly more accurate results than the common and the state-of-the-art practices, without requiring the MSUs to be calibrated, rendering the network to be self-calibrated. To achieve this, some assumptions on the error behaviour were made (i.e. additive, zero mean error). While these assumptions are commonly accepted, we have also presented a simple logarithmic data re-scaling technique, which enables the method to handle multiplicative errors. Therefore, generalising the suggested scheme even further.

In parallel to the implementation of the calibration procedure with Artificial Neural Networks (ANNs), an alternative ANN approach for calibrating the measurements was exercised in the Belgrade case study, to account for nonlinearities due to meteorological effects and interfering gases influence. A feed-forward neural network with one hidden layer consisting of 10 nodes ("nuerons") was used to calibrate the CO, O_3 and PM measurements of the DNET and AQMesh nodes. Training of the neural networks was carried out by using three different methods: 1) Levenberg-Marquardt algorithm (LM), 2) Resilient backpropagation algorithm (RB), and 3) Conjugate Gradient Powell-Beale algorithm (CG), based on 70% of the total number of measurements, 15% for validation and 15% for testing.

It was found that the ANN calibration outperformed the Multivariate Linear Regression (MLRs) approach, where the usage of explicit models with appropriate transformations is necessary. The LM ANN was found to yield the best results compared to RB, CGPB and MLR.

Portable Units

The CITI-SENSE project examined two “types” of mobile sensor measurements: using the nodes that were used for stationary measurements while there were mounted on vehicles, thus collecting data while moving, and using specially designed personal sensor nodes that can be “wear” while performing daily activities. We first describe the first approach, which was later abandoned by the project, while focusing on the second option.

Mobile nodes

The small size and low power-consumption of the AirBase nodes enabled to test them during mobile measurements. Placing such nodes on mobile platforms enables the coverage of a wider area with a smaller number of nodes, while keeping the spatial and temporal resolution high. Few recent studies showed the possibility and advantages of such a mode, based on the relatively easy adaptation of the nodes to function as mobile sensing units when they contain a GPS (Al Ali et al., 2010; Devarakonda et al., 2013). However, all these studies assumed that the motion itself has no effect on the sensors' performance. An attempt to consider this issue was done by Levy et al. (2014), using reference devices mounted in a van. Their study showed that a correction has to be applied to particulate matter measurements taken while moving, due to non-isokinetic sampling effects. However, they did not report any correction to the gaseous pollutants, since the instruments used had a regulated flow rate rather than diffusion-based sensors (passive samplers), as used in WDSN sensor nodes. For testing the effect of the motion of the sensors on the sensing performance, we used AirBase nodes equipped with metal oxides gaseous pollutant sensors. When the sensor faces the wind or the airflow due to the motion an increased heat transfer occurs at the sensors' face, which is known to affect its behavior (Honicky, 2011) since metal-oxide (and electrochemical) sensors required temperature stability for reliable measurement. Variations of the surface temperature, e.g. due to increased convective heat transfer, alter its current/voltage output. Wang et al. (2010) showed that metal-oxide gas sensors are sensitive to both ambient temperatures and relative humidity (RH), two variables that were found to be affected by the traveling speed, as shown below. Here, we report the performance of measurements made by sensors that travel at different velocities by comparing mobile and stationary measurements taken at the same time and location (Lerner et al., 2015).

The first stage of this study was done in a wind tunnel, aiming at quantifying the effect of the wind velocity in a controlled environment, with no local emission sources (e.g. traffic). At zero wind speed as well as under wind conditions but when all the nodes were shielded (unexposed to the wind) the sensors reported similar measurements. A clear change in the measurements was observed when the wind tunnel was turned on and the wind speed increased, with all the sensors (shielded and unshielded) reporting much lower NO_2 concentrations. This measurement artefact vanished once the air velocity (wind) ceased, after adjustment period of ~20-30 min. In fact, wind-derived temperature effect is so pronounced that the higher the wind velocity is, the lower is the variance of the measurements. The orientation of the node with respect to the airflow was found to have small (and non-significant) role on the sensor measurements. The O_3 measured values as a function of wind speed and node orientation (facing forward (F) or backward (B) relative to the airflow) are presented in Figure 10. The effect of velocity on the measurements is shown through the mean ratio of the shielded (C) to the exposed (E) nodes. It is clearly seen that as the wind velocity increases, the ratio increases. Thus, the forward-facing sensor reported higher concentrations of O_3, which is opposite to the effect of the wind on the NO_2 sensor (where higher wind speeds diminished the measurements).

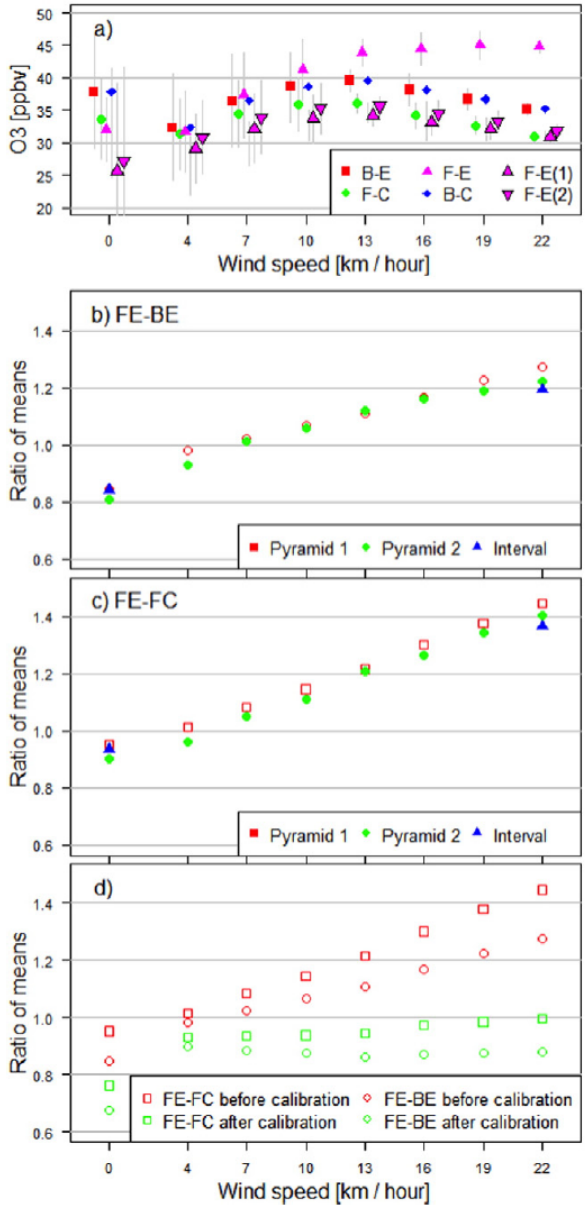

Figure 10. O_3 wind tunnel measurements by metal oxide sensors of the AirBase platform. (a) O_3 measured levels, (b) FE/BE and (c) FE/FC concentration ratios, and (d) FE/BE and FE/FC before (red) and after (green) correcting for the wind speed effect.

As seen in Figure 10, the ratio of measured values acquired by a sensor that was exposed to the wind and a sensor that was shielded from it were found to be linearly correlated with the wind speed, thus providing a simple means to correct the measurements for the speed of travel (in case of mobile nodes).

The second stage of this work was done in the field. The noise and temperature measurements were clearly affected by the motion (and orientation) of the nodes. Namely, with increasing velocities a higher noise level was measured, as could be expected from basic physics principles. Similarly, higher velocities affected to a greater degree the heat transfer from the sensor face, forcing lower temperatures than the ambient temperatures measured by stationary sensors. This result was consistent with the results obtained at the laboratory. RH measurements did not reveal consistent

effect of the sensors' traveling speed. Ozone and NO_2 measurements by sensors positioned perpendicular to the car's traveling direction showed no coherent effect of the vehicle speed. However, sensors that faced the travel direction were affected by the vehicle speed, with a four-to-fifteen-fold alterations to the measured values during travel.

Field Assessment of Sensor Platforms

Four platforms were evaluated under ambient conditions by comparing measurements with reference instruments at UCAM over varying length of time ranging days to months. Except for the Ateknea nodes, which are intended for personal exposure studies, the rest of the platforms were designed to be deployed as static nodes both indoors (AS) and outdoors (AQMesh and CVUT).

Inter-comparison in the field

Figure 11 and Figure 12 show results of inter-comparisons for temperature and CO over 5 days in August, 2014. 'K30_CO2' temperature is not part of the CITI-SENSE instrument but is co-located in the chamber with the CVUT instrument to reveal the expected difference between indoor and outdoor temperature.

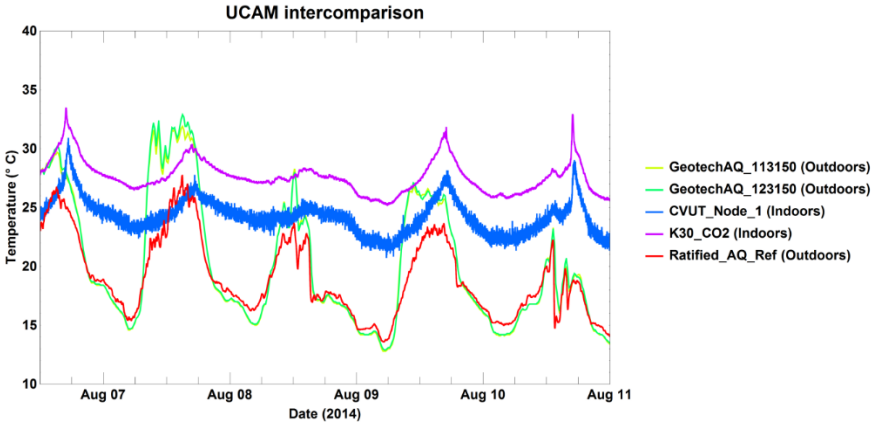

Figure 11. Time series comparing temperature measurements from different platforms to measurements from reference instrument (in red).

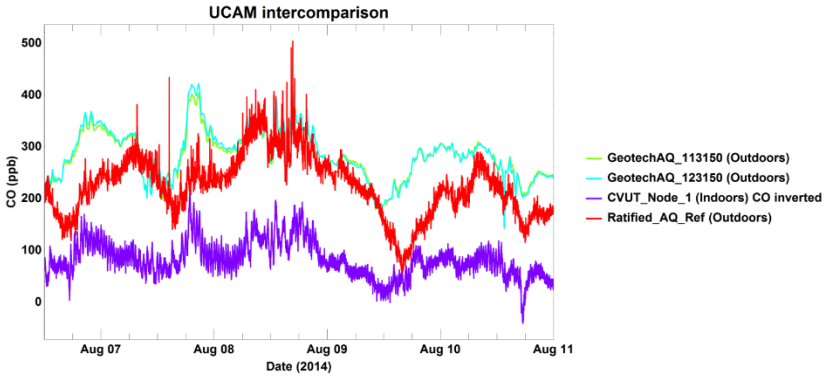

Figure 12. Time series comparing CO measurements from different platforms to measurements from reference instrument (in red).

Field assessment: Environmental Instruments / AQMesh pod

Results presented here are for a v3.5 AQMesh pod. Except for PM_{10} (R^2=0.5), overall there was good correlation ($0.74 < R^2 < 1$) for non-gaseous measurements ($PM_{2.5}$ and meteorology data). CO and O_3 comparison showed relatively good correlation with R^2 ~0.6 (Figure 5 and Table 2). Although the gradients of the PM measurements were very low, the good correlations suggested that the data could be calibrated using a single correction factor. NO_2 showed poor correlation with reference measurements, with R^2=0.36 and gradient of 1.6.

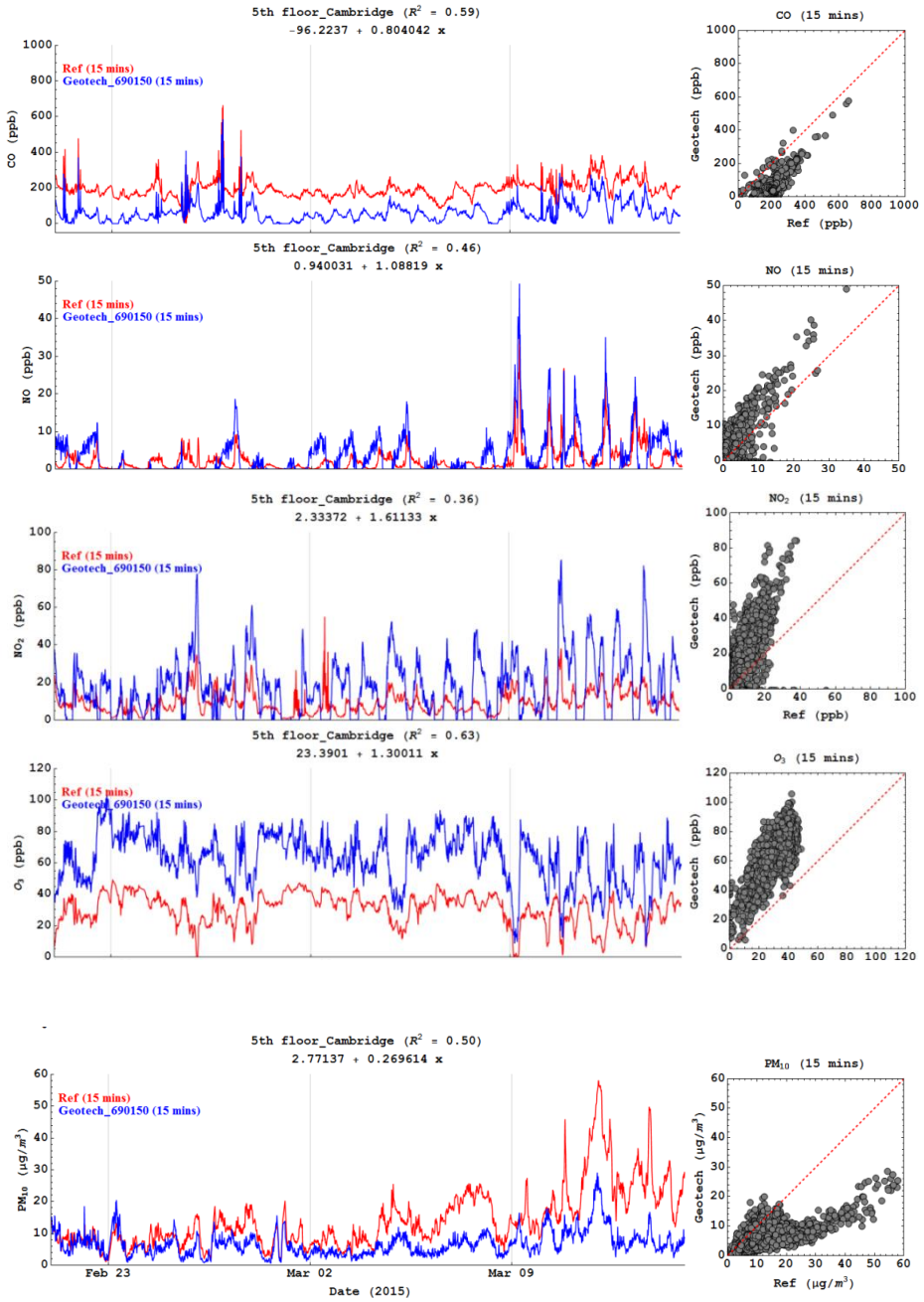

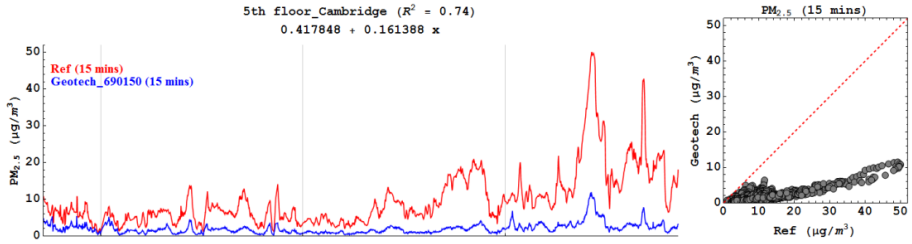

Figure 13. Time series and correlation plots of CO, NO, O_3 and NO_2 mixing ratios as well as PM10 and PM2.5 concentrations from the reference instruments and a AQMesh pod. Data covers 23 days (21 February to 15 March, 2015).

Field assessment: Ateknea units

Two prototype Ateknea personal monitors (A0AD and 9D3B) were studied in Cambridge. These units were not designed to be weatherproof hence were deployed in weatherproof enclosures for this comparison. Parameters recorded include NO, NO_2 and O_3 as well as temperature and RH at sampling rate of 20 s (user defined). Figure 14 indicates that the mixing ratio over the comparison period were very low at the sampling site, making it challenging to conduct meaningful comparison. In addition, there was non-systematic clock drift in the Ateknea units, which may also explain the poor correlation, especially for O_3, RH and temperature where the time lag between the reference and Ateknea node is obvious (Figures 14-15).

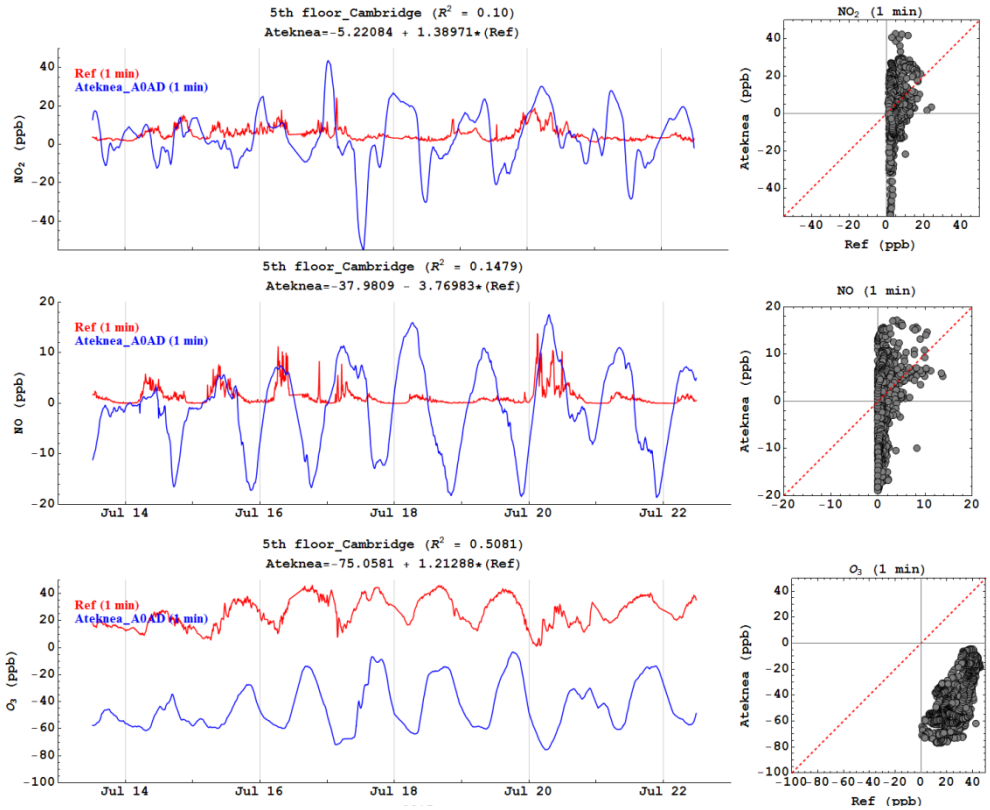

Figure 14. Time series and correlation plots of NO_2, NO, and O_3 mixing ratios measurements from the reference instruments and one of the Ateknea nodes. Data covers 10 days (13 – 22 August, 2015).

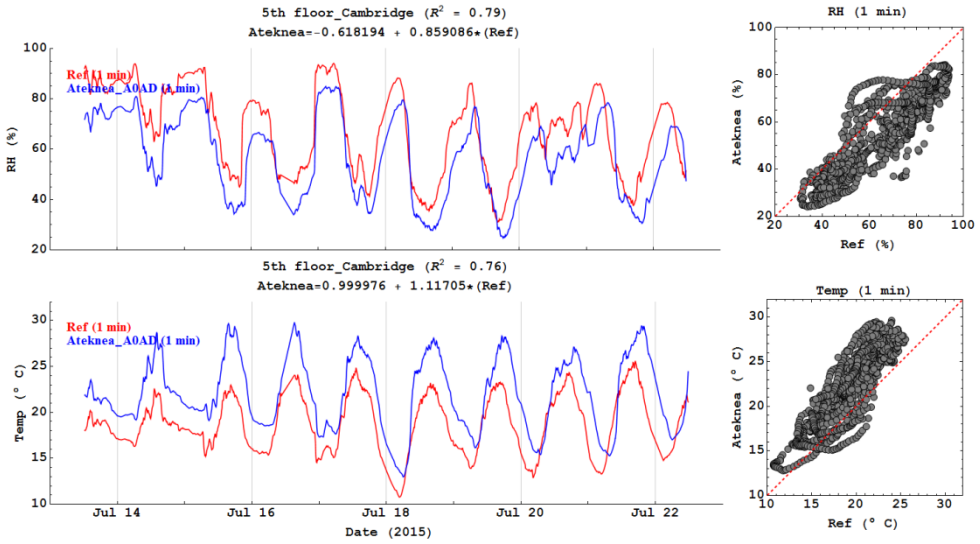

Figure 15. Equivalent plots to figure 6 for temperature and RH measurements.

Field assessment Atmospheric Sensor nodes

Two AS units (node 20 and 24) have been assessed outdoors in Cambridge since 30th May 2015 until 31th August 2015. This platform measures CO, NO, NO_2, O_3, total VOCs and CO_2. Other parameters include temperature, RH, sound and particulates (PM_1, $PM_{2.5}$ and PM_{10}). Data from these units are recorded every 5 min and comparison will be on this time scale. Unlike the AQMesh pod, the AS units provide both the raw data in volts and the on-board converted data for the toxic gas measurements based on Alphasense algorithm. There is an added advantage that once a final algorithm has been agreed, historical raw data can be re-analysed. The gas measurement comparisons presented are based on conversion using UCAM generated algorithm which AS will attempt to reproduce on their units. Figure 16 shows the time series and correlation plots for CO, NO, NO_2, O_3 and CO_2. There is good correlation for O_3 (0.7) and to some extent CO (0.42) and to a lesser extent for NO (0.33). However, the NO_2 and CO_2 measurements show low correlation with R^2 of respectively 0.26 and 0.20. Similarly, the PM correlations were poor especially for PM_{10} with R^2 of 0.14 (Table 13).

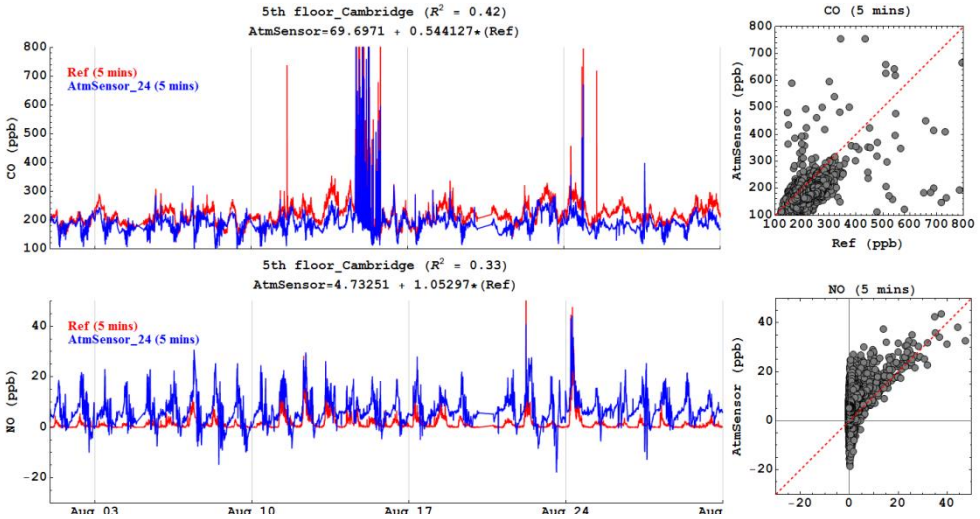

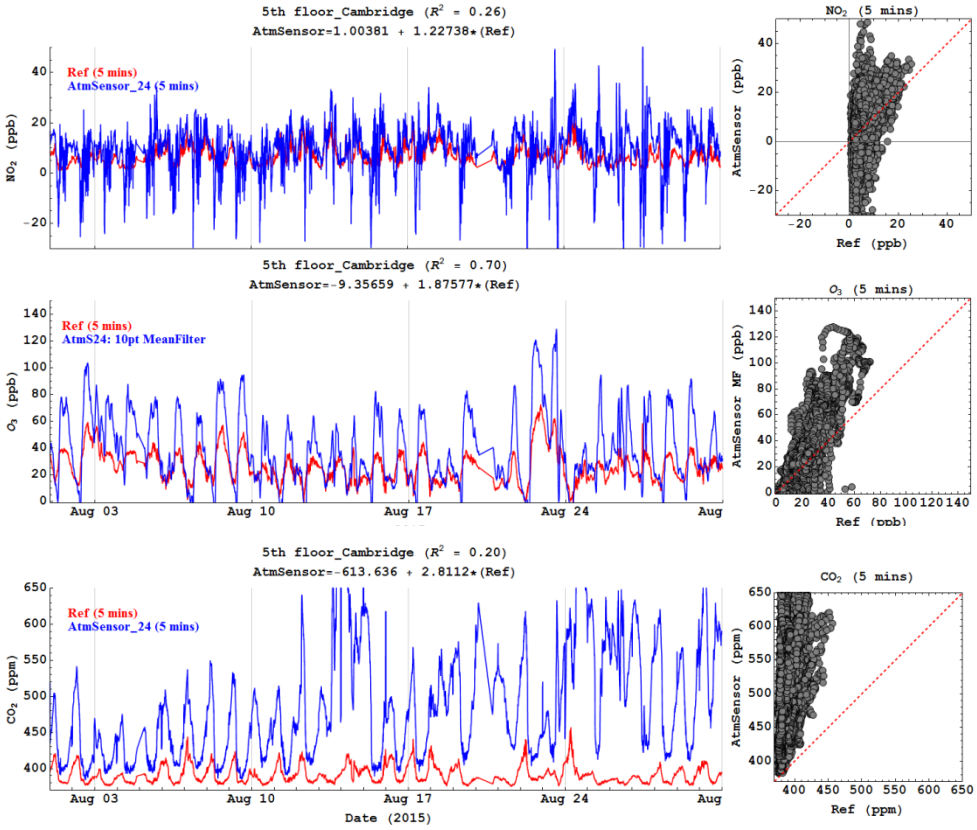

Figure 16. Time series and correlation plots of CO, NO, NO2, O3 and CO2 mixing ratios from the reference instruments and one of the Atmospheric sensor nodes. Data covers 31 days (1 to 31 August, 2015). Data produced using UCAM algorithm.

Field assessment: CVUT node

Although CVUT units were not selected as part of the final platforms to be used in the project, we have included their analysis in this report because it was fully assessed for ambient performance at UCAM. This node is not weather proof and was therefore deployed in a test chamber (Figure 2b) indoors, with common sampling inlet as the reference measurements. The CVUT instrument measured gas species (CO, NO_2, SO_2 and total volatile organic compounds, VOCs), as well as ambient temperature at a time resolution of approximately 14 s. These data were averaged to 1-minute resolution in order to match them up to the reference data that had time resolution of 1 minute. All the gas measurements were compared to reference measurements except VOCs, which is not measured at the reference station. Temperature measurements were also excluded from the comparison as the CVUT measurements were representative of laboratory rather the outdoor temperature recorded by the reference meteorology station. Figure 17 shows the CO, SO_2 and NO_2 time series and correlation plot of the mixing ratios for a month data (1 – 30 November, 2014) during the comparison period from September to December 2014. Except for CO that shows relatively good correlation (R^2=0.66), the comparisons were poor for the other gas species. Several factors may account for the observation, including low mixing ratio measurements at the site especially for SO_2, which are generally below 5 ppb. It is also possible that there were gas losses on the inlet system, reducing values of the comparison. However, the NO_2 measurements from the CVUT are over estimating the true measurements as shown in the summary in Table 13.

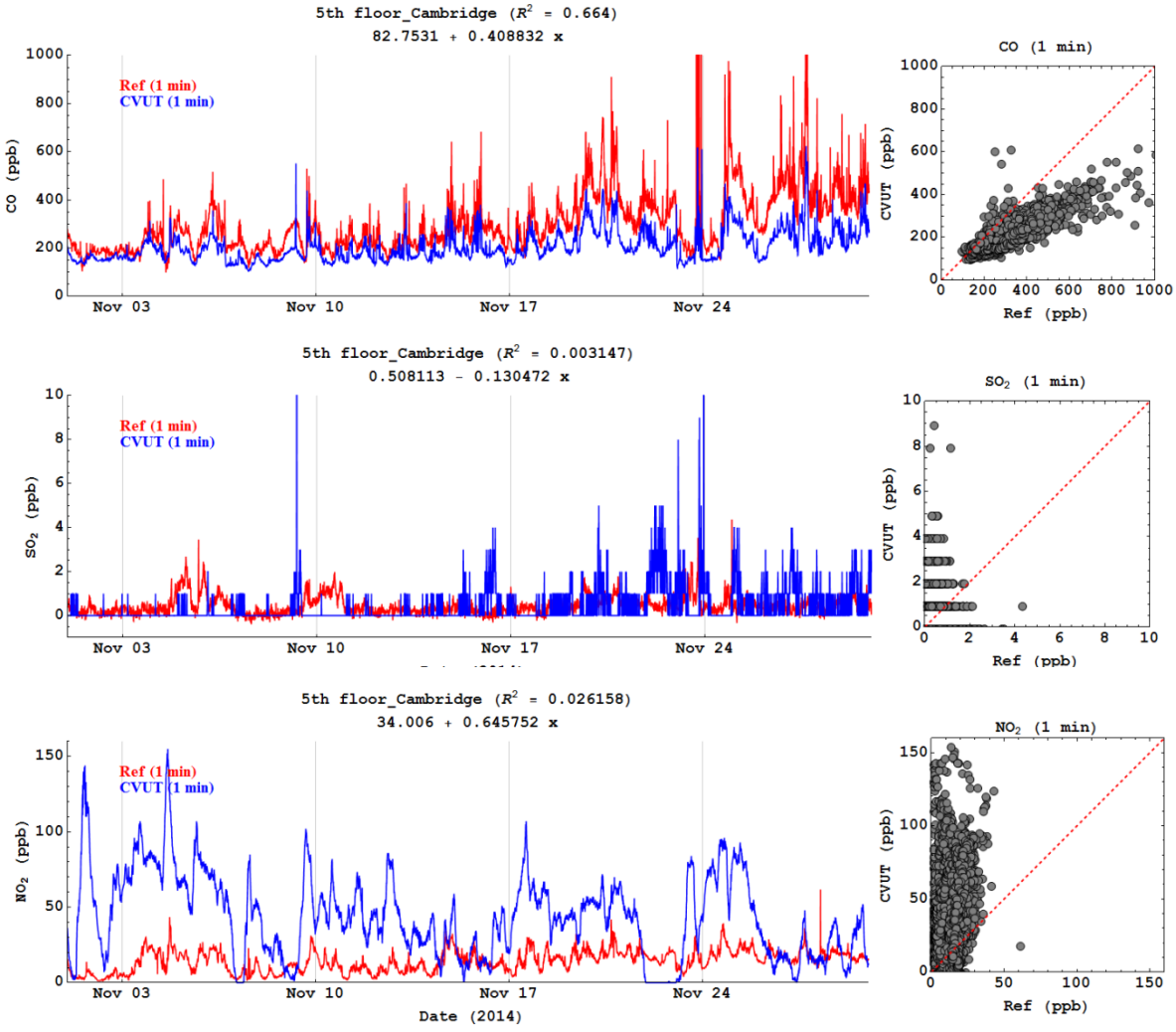

Figure 17. Time series and correlation plots of CO, SO2 and NO2 mixing ratios from the reference instruments and a CVUT node. Data covers 30 days (1 to 30 November, 2014).

Overview of Field Performance of the Platforms

Table 13 summarise the statistical data of the field comparison for all parameters compared for each platform with measurements at UCAM monitoring station. We found that all platforms were able to reproduce meteorological measurements like RH, ambient temperature and atmospheric pressure (when measured) to within 5-20% of the reference measurements. However, the performance was different for gas and particulate measurements. We observed some agreements for CO (R^2 =0.42-0.66) and NO (R^2 =0.15-0.46) and encouraging results for O_3 (R^2 =0.51-0.70), all subject to proper re-calibration of the data. NO_2 (R^2 =0.1-0.36) showed the least correlation with the reference measurements. While the NO_2 sensors show good performance under controlled conditions (as presented in the laboratory data comparison evaluation at NILU). These results reinforce the challenges in reproducing such level of performance in ambient condition. It is noteworthy that the mixing ratios at the monitoring station for NO_2 were often low, generally below 40 ppb, making any error associated with temperature more significant at these levels. Previous studies in Cambridge 2009 and more recently at London Heathrow airport using similar electrochemical sensors close to ground level have shown good agreement (R^2 =0.8-0.9) for O_3 corrected NO_2 data. Thus with improved temperature compensation algorithm on these new generation NO_2 sensors, there was a strong

indication that acceptable indicative NO_2 measurements at street levels can be achieved. The PM measurements were overall encouraging in the AQMesh units, especially for the number concentrations. In contrast, there is a strong indication that the PM measurements in the AS nodes are affected by RH, which results in poor correlation (R^2 =0.14-0.31) with the reference data. Though the current measurements can be used to indicate relative PM exposures, efforts have to be put into compensating for this effect to possibly extract quantitative PM information. CO_2 data were only measured by the AS nodes, though there appears to be strong baseline and sensitivity drift with time, these can be quantified and the data retrospectively corrected.

Table 13. Summary of linear fit metrics for three platforms (AQMesh, Ateknea, Atmospheric and CVUT sensor nodes) when compared to reference measurements.

Platform	Duration of comparison (days)	Species/ parameter	Pearson correlation (R^2)	Gain	Intercept	Data Average Time (minutes)
AQMesh	23	CO	0.59	0.80	-96 ppb	15
		NO	0.46	1.10	0.94 ppb	
		NO_2	0.36	1.61	2.33 ppb	
		O_3	0.63	1.30	23.3 ppb	
		Temperature	0.97	1.11	-0.85 ° C	
		RH	0.96	0.78	14.8 %	
		Pressure	1.00	0.99	7.68 mBar	
		$PM_{2.5}$	0.74	0.16	0.42 µg/m^3	
		PM_{10}	0.50	0.27	2.77 µg/m^3	
		PM count	0.74	0.006	0.425 N/cm^3	
Ateknea†	10	NO_2	0.10	1.39	-5.22 ppb	10
		NO	0.15	-3.77	-38.0 ppb	
		O_3	0.51	1.21	-75.1 ppb	
		RH	0.79	0.86	-0.62 %	
		Temperature	0.76	1.12	1.00 ° C	
Atmospheric sensors§	31	CO	0.42	0.54	69.7 ppb	5
		NO	0.33	1.05	4.73 ppb	
		NO_2	0.26	1.23	1.00 ppb	
		O_3	0.70	1.88	-9.36 ppb	
		Total VOCs	NA‡	NA‡	NA‡	
		CO_2	0.20	2.81	-613 ppm	
		Temperature	0.94	1.23	-2.73 ° C	
		RH	0.96	1.14	-12.3 %	
		Sound	NA‡	NA‡	NA‡	
		PM_1	0.31	2.45	-6.37 µg/m^3	
		$PM_{2.5}$	0.31	5.45	-23.2 µg/m^3	
		PM_{10}	0.14	4.15	-20.4 µg/m^3	
CVUT	30	CO	0.66	0.41	83 ppb	1
		NO_2	0.026	0.64	34 ppb	
		SO_2	0.003	-0.13	0.5 ppb	

‡ There is no corresponding reference data for comparison, statistics represented as NA.

† Though the data here had been post processed by Ateknea to account for the time drift, the 2-minutes averaged data provided still present same issue. Ten minutes averaged data were used for the comparison with the reference station.

§ The atmospheric sensor EC data were calculated using UCAM algorithms rather than the new algorithms provided by Atmospheric Sensor

ANNEX I

Stationary Sensor nodes

Table A1. Characteristics of Static Sensor Platforms

Provider	Length x Width x Depth (mm)	Weight (Kg)	Communication	Temperature Range
Airbase	85 x 135 x 60	3	GSM/GPRS	-40°C to +85 °C
CVUT	120 x 120 x 100	0.5	GSM/GPRS(Master) – ZigBee (Slave)	N/A
DuvaNET	225 x 150 x 100	0.5	GSM/GPRS	-30 to +50 °C
AQMesh	150 x 180 x 200	2	GSM/GPRS	-20°C to +40°C
OBEO	120 x 124 x 44	0.2	GSM/GPRS	5°C to 35°C

AirBase

Airbase provided static sensors for WP3b. The specifications of CanarIT AirBase's platform are:

- CO_2/O_3, NO_2, VOC, TSP (ppb), Temperature (°C) & Relative Humidity (%), Noise.
- Electrical specifications: Power: 12V DC, Current Drain (@12V): 600mA, Power Adaptor: (inclusive): 12V DC, 250mA or more, 2.1mm plug, center pin positive (power adopter is included).
- The device sends a packet of measurements data to the server every 20 seconds using a GPRS connection.
- Metal box

Figure A1. CanarIT Sensor Platform.

CVUT

CVUT used an ad-hoc network architecture for their provided sensor platforms. A master node and slave nodes have been designed. The master station is static mountable box with following features:

- SO_2, NO_2, CO and VOC sensors, Alphasense A4 family electrochemical types, mounted on Alphasense AFE Board.
- Dust sensor providing two signal: particles less or equal to 2.5 µm, particles greater than 2.5 µm (can be filtered to limit upper size of particles)
- Power supply possibilities with following options: Internal 6600mA Lithium-Ion battery charged either from an external power input or a solar panel, 72 hour autonomy of sensor unit is expected. Battery voltage is sensed and communicated to the server; External power supply 7 to 40 V connected via external IP68 connector; Solar panels for charging (optional use)
- GSM/GPRS module for GSM communication of master node with the central server; 802.15.4 module for communication of master node with slave nodes;
- GPS module used for location information of every master node.
- MicroSD slot for insertion of memory card. Data from the SD card may be uploaded to the FTP server upon remote request or in case of necessity;
- Weather resistance, ease of installation and intrusion detection (accelerometer), motion detection via GPS and accelerometer; Automatic firmware upgrade over the air; Event - driven behavior of the control system
- Non-flammable plastic box equipped with filtered input air ventilation to the sensors. Two fans are used for individual suction: one for the gas sensors and the other for the dust sensor. These fans are individually controlled by internal electronics.

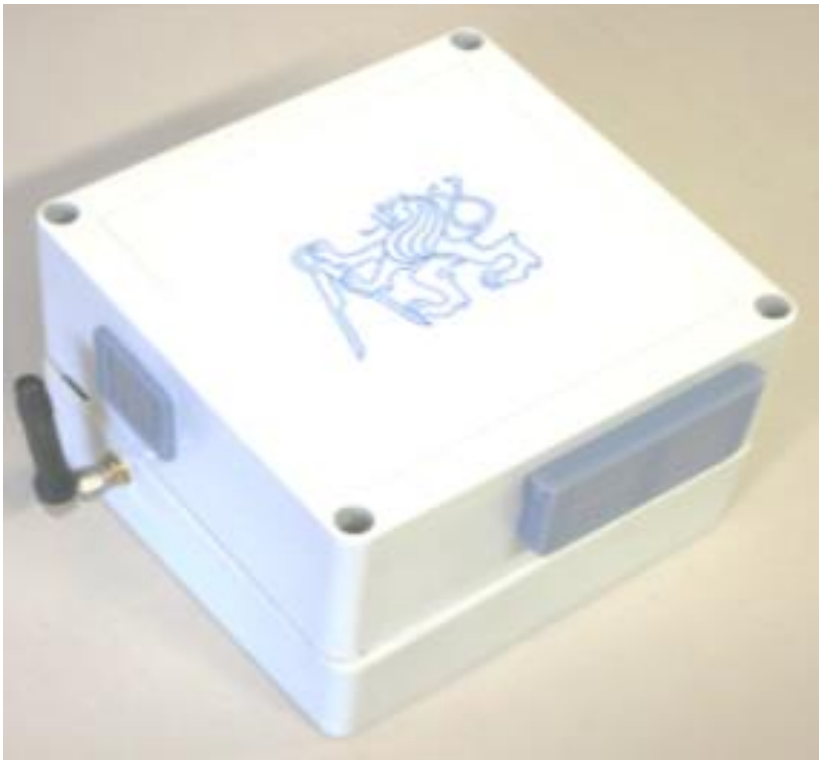

Figure A2. Master node with vents / filters

AQMesh

The AQMesh Pod for the pilot test contains measurement capabilities of the following:

- Gases NO, NO_2, O_3, CO (ppb)
- Pressure (mB), Temperature (°C) & Relative Humidity (%)
- The Pod is powered by a battery with an outline performance.
- The data is collected from the sensors and transmitted via GPRS to a secure server for processing. Then the data is post-processed and the correction algorithms are applied.

Figure A3. AQMesh with Sun Protection.

DNET

The ekoBUS700++ device is designed for vehicle mounting, and measures air pollution and atmospheric conditions at the location of the vehicle (with vehicle location determined by a built-in GPS module). It can also be located at fixed indoor/outdoor locations to monitor local environment parameters. Gas sensors are Alphasense B4 family electrochemical types and IRC-A1 for CO2 (Infrared). T+%RH is Sensiron SHT11. Air pressure sensor is MPXA6115AC6U.

- CO_2, O_3, NO-B_4, NO_2-B_4, SO_2-B_4 ,CO-B_4
- MPX4115 (15 - 115 kPa)
- SHT71 (-40°C – 123°C, 0-100%)
- It is a possible to connect external devices and additional sensors via USB or RS232 communication ports on the EB7000++. A Dylos DC 1700 device for Particulate Matter measurements is integrated with EB700++, and communicates via the RS232 port. Measurements obtained from this sensor are also sent by the EB700++ device to the back-end server.
- The collected measurements are transferred to the back-end server via GPRS where they are stored and further processed.
- Robust industrial housing, depends on indoor or outdoor usage. For indoor usage, the EB700++ is housed in an aluminium enclosure. For outdoor installations, the EB700++ is mounted in a waterproof PVC box with two pipes for air circulation.

Figure A4. EB700++ Device Mounted in a Box for Outdoor Usage.

OBEO

OBEO provides an indoor radon sensor with GSM conectivity. The Obeo MMR is a radon sensor for indoor use with quad band GSM/GPRS capabilities and built-in antenna.

- A silicon semi-conductor detects Alpha Particles. This detector is encapsulated by a positively charged housing (metering cell).
- The data is collected and stored in memory and is uploaded to the central Citi-Sense server, over GSM cellular network at intervals of twelve hours.
- The MMR is supplied with an external AC/DC adapter for 230VAC use. The adapter comes with various inserts, allowing it to be compatible with all types of mains outlets.
- The MMR features an in-house designed ABS enclosure. All of the electronics, including the radon detector circuitry is developed by Obeo.
- Resolution - 1 Bq/m³

Figure A5M. MR top view

Mobile / Personal Platforms

As mentioned above highly portable sensor platforms have been designed. These platform have been designed to be used with a commercial smartphone. These were designed to be ultra-compact, lightweight, robust and battery powered, to be conveniently worn/carried, or accompanying the user in daily life, and supporting multiple environmental sensors. The smartphone's internal sensors are being used to provide complementary environmental and data: e.g. GPS (for position), motion sensors (for activity). The smartphone provides the gateway to the Citi-Sense data and services platform.

Table A2. Characteristics of Portable Sensor Platforms

Provider	Length x Width x Depth (mm)	Weight (gr)	Communication	Temperature Range
ATEKNEA	85 x 135 x 60	3	USB and BT2.0	-40°C to +85 °C
JSI	32 x 100 x 210	270	USB, BLE or Wi-Fi	-25°C to +50°C

ATEKNEA

The Little Environmental Observatory (LEO) is equipped with the following sensors:

- NO_2, O_3, CO (ppb) - Alphasense B4 family electrochemical types, each one with Alphasense Individual Sensor Board (ISB)
- Temperature (°C) & Relative Humidity (%) – (Sensirion SHT75)
- USB and Bluetooth 2.0 communications using a smartphone as gateway to send data to a remote server.
- Internal 1300mA Lithium-Ion battery. The battery is charged via the USB port (expected 72hr autonomy of sensor pack)
- Sensor pack electronics, sensors and battery are housed in an ABS plastic box, which is then inserted into a black textile pouch with a zip. The pouch contains a Velcro strap to facilitate attachment to a belt or harness etc.
- The sensor pack is designed to work with an android smartphone. The Smartphone App is being developed by WP7 partner S&C. The smartphone will provide GPS position, and user activity data and form the communication gateway between the sensor pack (via Bluetooth) and the server (via GPRS etc.).
- For communication via USB: ATEKNEA supplies a simple monitor program to enable download of sensor pack data and saving in .CSV format, which can then be imported into a spread sheet.

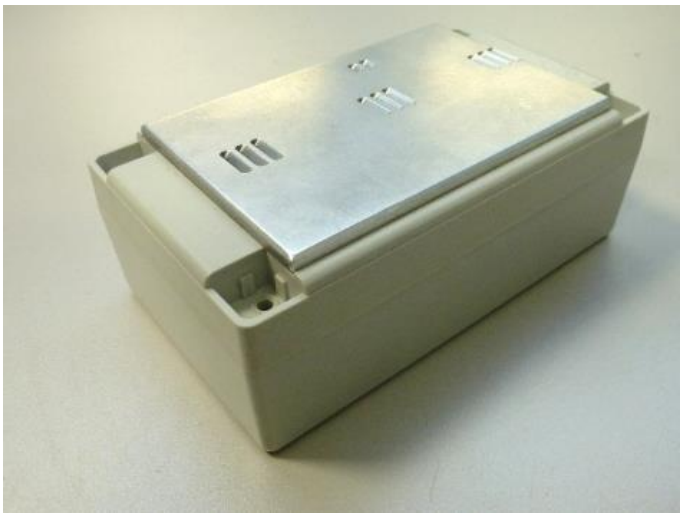

Figure A6. Personal Sensor Pack Assembly (ATEKNEA)

Based on the feedback from WP2 and the tests performed at NILU, ATEKNEA has redesigned its Portable Sensor Pack (PSP). The electronics of the unit was reduced in size integrating the A4 Series electrochemical sensor from ALPHASENSE (including the new versions of O_3/NO_2). This reduction allowed for a smaller form factor making the new sensor platform almost half the size of the old one (Figure A7). The new version came with an arm strap and a belt clip, so that users could chose to wear the sensor in the most comfortable way. The old mechanical design (with aluminium plate) affected the performance of the O_3 sensors, feedback from NILU has been taken into account for the redesign of the new unit. The gas sensors now are closer to the wall of the enclosure, improving airflow for better performance. Two temperature sensors were used in the new PSP. The first one (a PT1000 provider with ALPHASENSE AFE board) is used for temperature compensation, and the second one (Sensirion SHT11) is used to measure actual ambient temperature and relative humidity. Furthermore, the microprocessor in the new PSP unit was upgraded improving the performance and stability of the communication with the Smartphone via Bluetooth.

Figure A7. ATEKNEA's new Portable sensor Platform

A more detailed comparison between the old unit and new unit can be appreciated in Table A3. Regarding the app for the smartphone Sensing & Control (S&C) has been upgrading the APP2 based on requirements from EIs and new features provided by ATEKNEA. Some of these include:

- Processing of RAW sensor data, to provide the measures in the correct units. This includes the integration of the temperature compensation algorithm for the gas measurements.
- Addition of debugging functions for troubleshooting of communication with the PSP.

Table A3. Pilot and Full Deployment Platform Comparison (ATEKNEA Joeys)

Features	Phase 1	Phase 2
Gas Sensors		
O_3	Alphasense B4 Series (ppb)	Alphasense A4 Series (ppb)
NO_2	Alphasense B4 Series (ppb)	Alphasense A4 Series (ppb)
CO	Alphasense B4 Series (ppb)	Alphasense A4 Series (ppb)
Gas Interfaces	Alphasense B4 Board	Alphasense AFE 3-way Board
Other Sensors		
Temp (ambient)	N/A	Sensirion SHT11
RH (ambient)	N/A	Sensirion SHT11
Temp (internal)	Sensirion SHT75	PT1000 on AFE Board Alphasense
RH (internal)	Sensirion SHT75	N/A
Enclosure		
Dimensions (L x W x D) mm	85 x 135 x 60	80 x 96 x 44
Volume (cc)	669	338
Material	ABS + aluminium plate	ABS
Total Weight (gr)	270	200
Protection Rate	IP51	IP64
Extras	Pouch, Interior cotton canvas fabric, Exterior polyester canvas fabric	Arm band, or belt/pocket clip
Communications		
With Server	Through smartphone via Bluetooth	Through smartphone via Bluetooth
With PC	USB	USB
With Smartphone	Bluetooth 2.0	Bluetooth 2.0
Battery		
Type	Lithium-ion	Lithium-ion
Specifications	3.7V-1300mA	3.7V-950mA
Autonomy	32 h	29 h
Charger	5V @ 500mA (micro USB)	5V @ 500mA (micro USB)
Main Power		
Platform Input Power	N/A	N/A
Volt	N/A	N/A
Power	N/A	N/A

JSI

The VESNA-based personal sensor unit is equipped with the following sensors:

- NO_2, O_3, CO (ppb)
- Temperature (°C) & Relative Humidity (%) – (Sensirion SHT21)
- Accelerometer – Freescale MMA8453Q
- Personal sensor unit supports wireless connection to an Android smartphone and/or tablet via Bluetooth Low Energy profile or Wi-Fi.
- The personal sensor unit is battery operated and includes 3 AA size rechargeable batteries providing 1300 mAh capacity. Charging of the battery is provided via micro USB connector. Expected autonomy of the personal sensor pack is in the range of 48 hours.
- The personal sensor unit is housed in a plastic box.
- For calibration purposes raw data can be downloaded via USB,

Figure A8. Top view of the VESNA Personal Sensor Unit

ANNEX II

Test Facilities for Pilot and Full Deployment

The quality of data generated during CITI-SENSE measurement campaigns was highly dependent on the performance of the micro-sensors/instruments collecting it. One of the tasks of WP8 was to evaluate the gas sensing instrumentation made available by the Platform Providers within WP8. Despite an exhaustive characterization of these sensors being beyond the scope of the project, some preliminary quality control of the equipment is considered necessary and thus has been performed.

NILU

NILU's testing capabilities had the instruments that are listed in Table B. A gas calibrator associated with high-concentration gases was used to ensure satisfying gas concentration stability during the test. All high-concentration cylinders in use are traceable gas standards (National Institute of Standards and Technology - NIST or National Physical Laboratory - NPL).

Table B1. Gas Analysis and Dilution Instruments

Instrument type	Instrument	Measurement Method	Detection limit [ppb]
O_3 analyser	Teledyne API 400	Ultraviolet photometry	0.4
SO2 analyser	Teledyne API 100E	Ultraviolet fluorescence	0.4
CO analyser	Teledyne API 300E	Infrared absorption Gas Filter Correlation	300
NO_x analyser	ML9841B	Chemiluminescence	0.4
H_2S analyser	Teledyne API 101E	Ultraviolet fluorescence	0.4
Dilution system	Environics Series 100	Mass flow controllers	N/A

Testing Chamber: Chalmers-type Deposition Chamber

The testing setup consisted of three separate exposure chambers made of Pyrex glass (Figure B1). The three chambers were connected to the mixing chamber "M". All parts of the pneumatic circuit were made of either PTFE or glass. Each bottle of gas contained a volume of 10 litres. A thermostatic bath provided good thermal stability, even for long-term experiments. All testing gases run through rudimentary heat exchangers which were immersed in the bath. Relative humidity could be regulated from 0 – 90 %RH. A dedicated mixing chamber was connected to incoming sample gas and to vapour-saturated air provided by a humidifier. Regulation of each incoming flow allowed a precise control of the final sample relative humidity as well as constant gas concentration. Both temperature and relative humidity were accurately monitored in each chamber (Rotronic HygroClip probe to measure relative humidity and temperature.).

Most gases were generated by diluting high-concentration gases (NO, SO_2 & CO). The dilution unit was equipped with an internal O_3 generator which allowed production of both O_3 and NO_2. The latter was produced by mixing NO with O_3 (via Gas Phase Titration, GPT).

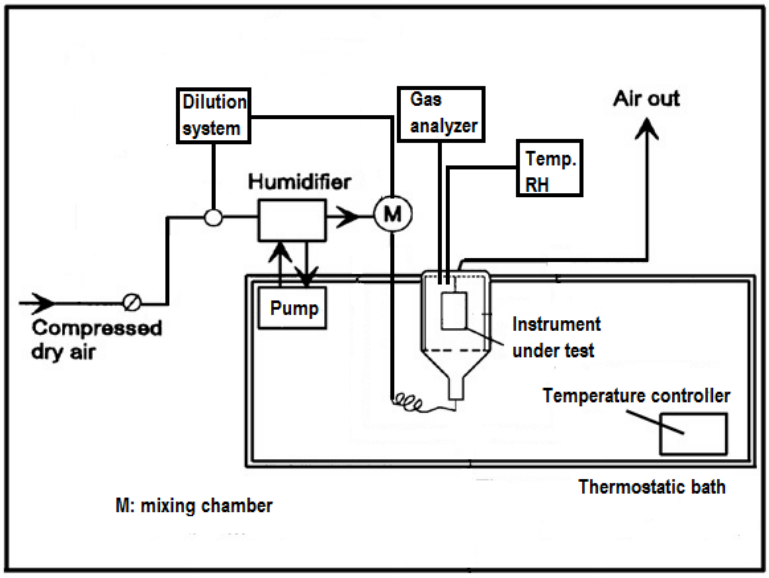

Figure B1. Description of Laboratory Setup at NILU

Test description

The laboratory tests consisted of multi-point calibration sequences performed with one gas at a time, at fixed temperature and relative humidity conditions. Each gas concentration level step consisted of 90 min. It should be noted that a full characterization of the platform performance was beyond the scope of this task.

UCAM

UCAM has setup a monitoring station comprising a suite of reference and equivalent instrumentations for continuous outdoor measurements of toxic and greenhouse gases, particulates and meteorological parameters. This monitoring site has been running from first quarter of 2014. Except for the weather station and particulate instrument, which are both located outdoors, all other instruments are housed indoors. All measurements are made on the roof of the Chemistry Department building in Cambridge UK (52.19761 N and 0.12529 E), located in the city centre close to a quiet road. Although the sampling inlet is approximately 22 m above mean sea level, long-term measurements will be influenced by both local and regional emissions.

The table below summarises different instrumentation used for the measurement of gases, particulates and weather at UCAM. The gas analysers were located indoor and fitted with a gas inlet line while the particulate and weather stations were outdoors.

Table B2. Instrumentation for gas species, particulates and weather

Instrument type	Instrument	Measurement method	Detection limit (ppb)
CO analyser	Thermo Scientific ® Model 48i CO Analyser	Infrared absorption, GFC	40
NO-NO_2-NO_X analyser	Thermo Scientific ® Model 42i-NO-NO_2-NO_X	Chemiluminescence	0.40
O_3 analyser	Thermo Scientific ® Model 49i O_3 analyser	Ultraviolet photometric	0.50
SO_2 analyser	Thermo Scientific ® Model 43i SO_3 analyser	Pulsed fluorescence	< 0.5
Zero Air Supply [a]	Thermo Scientific ® Model 111 analyser	Filter, scrubber, activated and heated reactor	N/A
Dynamic calibrator	Thermo Scientific ® Model 146i analyser	MFC (0 – 1000 sccm [d]) Output (0 – 10,000 sccm)	N/A
CO_2 and CH_4 analyser	Picarro ® G2201-i analyser	Cavity Ring-Down Spectroscopy (CRDS)	200 (12C) for CO_2 10 (13C) for CO_2 50 (12C) for CH_4 10 (13C) for CH_4
Particulate instrument [b]	Fidas ® 200 S	optical aerosol spectrometer: light Lorenz-Mie light scatter	
Weather station [c]	Lufft ® WS 600 Met station		±0.2°C (-20 to 50°C) ±2% RH ±1.5 hPa ±3°(WD) ±0.3ms^{-1}(WS) 0.01mm (precipitation)

[a] For NO, NO_2, O_3, SO_2 and CO.

[b] For $PM_{1.0}$, $PM_{2.5}$, PM_4 and PM_{10}.

[c] For wind speed, wind direction, temperature, humidity, pressure and precipitation

[d] sccm (standard cubic centimetre per minute)

Gas species measurement (instrumentation for Indoor testing)

Outdoor air is pumped through polyvinylidene fluoride (PVDF) inlet manifold (Figure B2) from which each analyser samples air via fluorinated ethylene propylene (FEP) inlet. Data are reported as 1 min average. In the sampling mode, the blue line in Figure B2 is in use. Zero and span calibration (red lines in Figure B2) are done daily just after mid-night, these data are subsequently used for ratification of the raw measurements. A standard gas cylinder mix containing 201 ppm CO (±2%) and 20.9 (±2%) ppm NO from Air Liquide, UK was used for laboratory calibration. A dynamic gas calibrator (Thermo Scientific Model 141i) was used to dilute the high concentration CO and NO gas using zero gas generated from Thermo Scientific Model 111 Zero Air Supply. Zero gases generated contain <0.1 ppm (CO and hydrocarbons), <0.8 ppb (O_3) and <0.5 ppb (NO, NO_2, SO_2, H2S and NH_3). All the analysers (Table 7) are serviced annually to ensure the desired precisions and accuracies are still achieved.

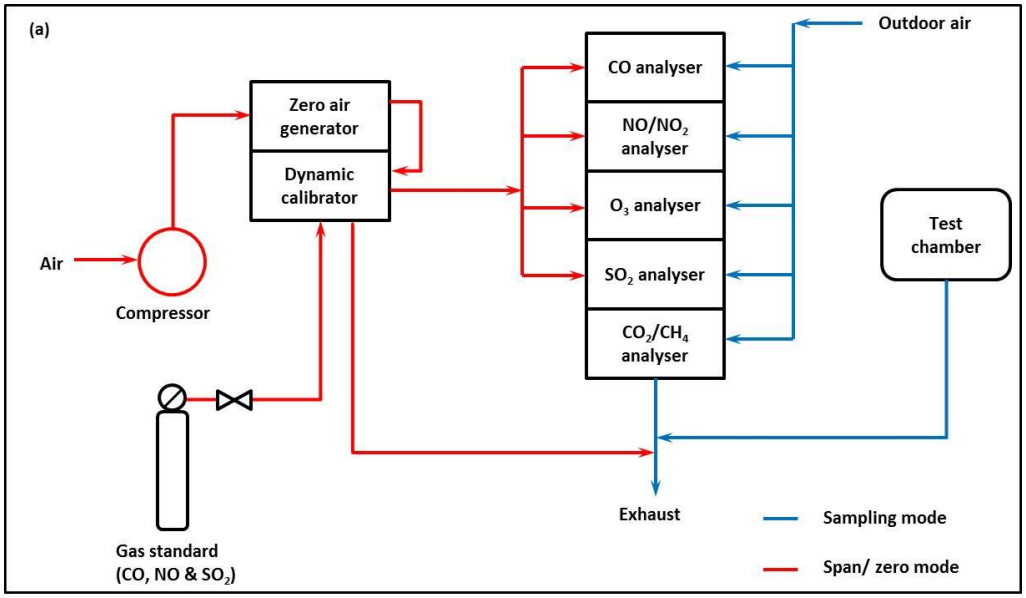

Figure B2. Layout of gas measurement (UCAM)

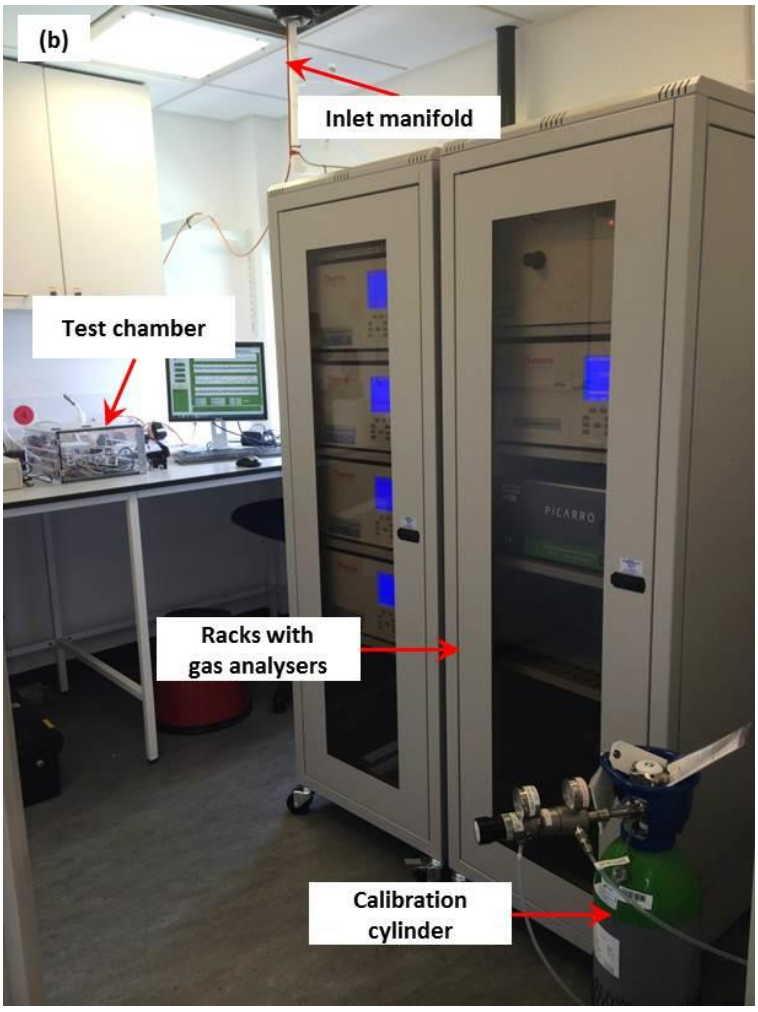

Figure B3. Layout of gas measurement (UCAM)

Particulate and Weather station (Outdoor instrumentation)

Both the particulate and weather instruments are located outdoors (Figure B4) close to the inlet manifold that supplies the gas analysers. Data from these two instruments are also reported as 1 min averages with the same timestamp as the gas measurements. This allowed comprehensive data analysis using varying environmental factors on all the gas species monitored. Field comparison can be done using test chamber located indoor (Figure B3) or by mounting weather-proof instruments outdoors (e.g. AQMesh pods, Figure B4). Figures B5 and B6 show example of a year and a week data recorded respectively by the gas analysers, PM instrument and weather station.

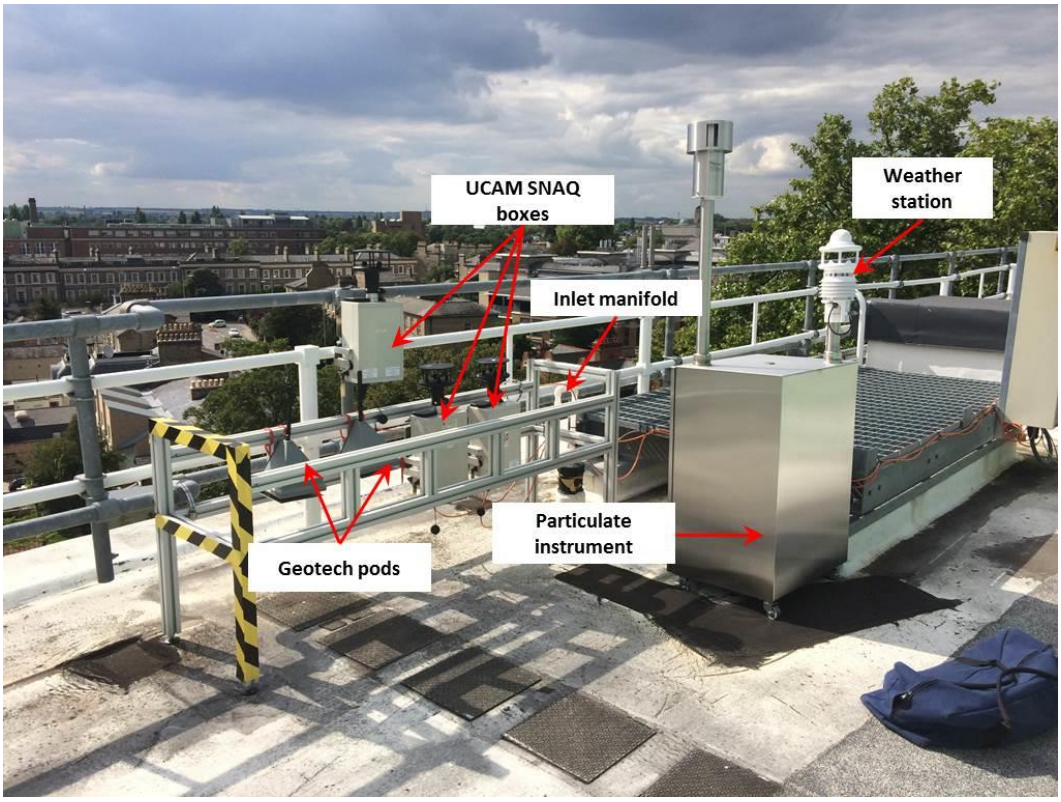

Figure B4. Weather station, particulate instrument and inter-comparison instruments (AQMesh pods and UCAM SNAQ boxes)

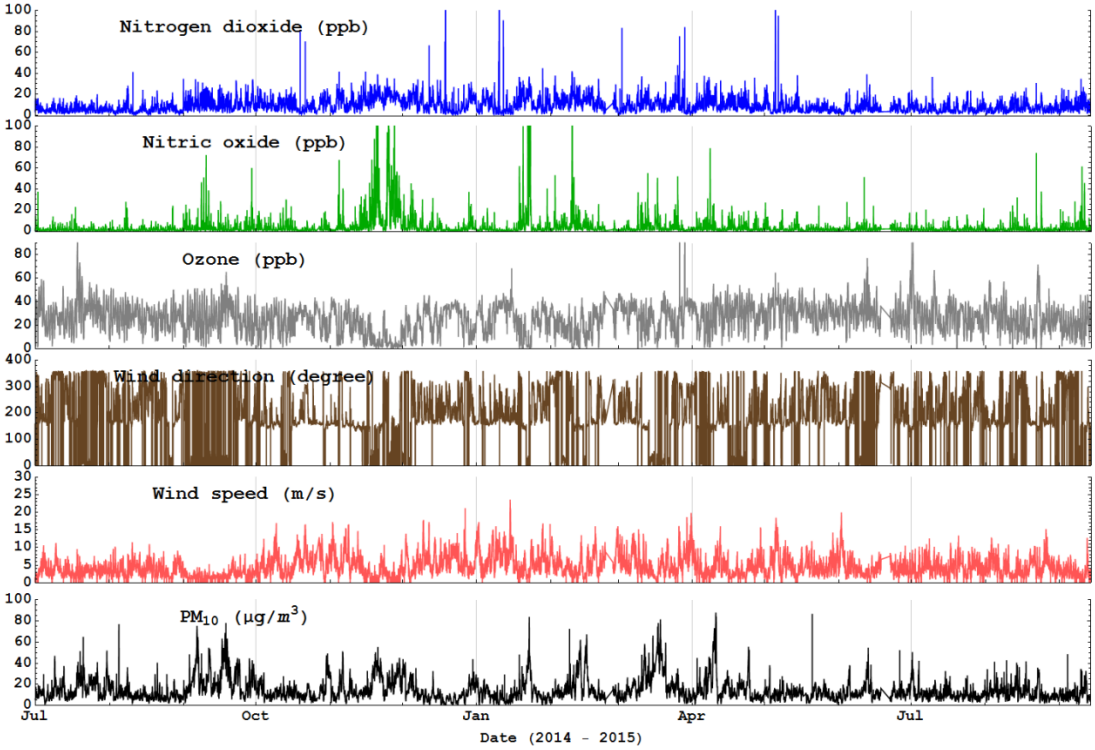

Figure B5. Time series of outdoor NO, NO_2 and O_3 mixing ratio, PM_{10} and wind measurements over a period of one year (July, 2014 to September, 2015).

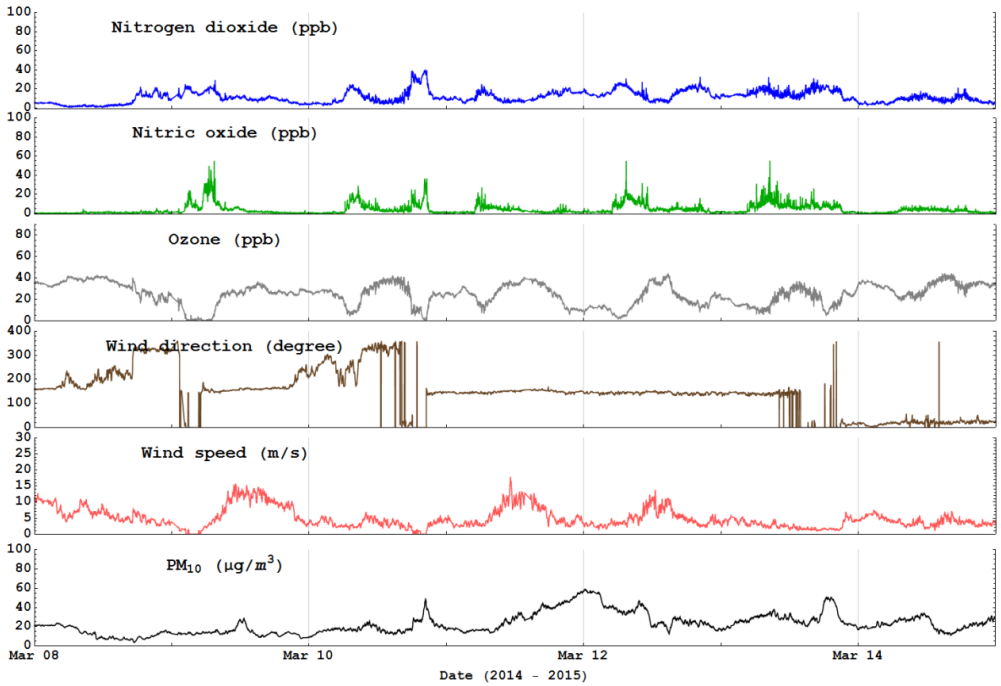

Figure B6. One week data (8 – 14 March, 2015) of outdoor NO, NO_2 and O_3 mixing ratio, PM_{10} and wind measurements.

Refrerences

Bard A., Faulkner L., Electrochemical Method: Fundamentals and Application, 2 ed., New-York, NY, USA: John Wiley & Sons, 2001.

Broday D.M., Rosenzweig R. Deposition of fractal-like soot aggregates in the human respiratory tract. Journal of Aerosol Science, 42:372-386, 2011.

Cai J., Yan B., Kinney P.L., Perzanowski M.S., Jung K.-H., Li T., Xiu G., Zhang D., Oliv, C., Ross J., Optimization approaches to ameliorate humidity and vibration related issues using the microAeth black carbon monitor for personal exposure measurement. Aerosol Sci. Technol., 47(11):1196–1204, 2013.

Carminati M., Pedalàa L., Bianchi E., Nasonb F., Dubini G.. Cortelezzi L., Capacitive detection of micrometric airborne particulate matter for solid-state personal air quality monitors. Sensors and Actuators A: Physical, 219:80-87, 2014.

Carminati M., Ferrari G., Sampietro M., Emerging miniaturized technologies for airborne particulate matter pervasive monitoring. Measurement, 2015.

Castell N., Dauge F.R., Schneider P., Vogt M., Lerner U., Fishbain B., Broday D., Bartonova A. Can commercial low-cost sensor platforms contribute to air quality monitoring and health exposure estimates? Environment International. 2016.

Fishbain B., Moreno-Centeno E., Self Calibrated Wireless Distributed Environmental Sensory Networks. Scientific Reports, 6:24382, 2016. DOI: 10.1038/srep24382

Fishbain B., Lerner U., Cole-Hunter T., Castell-Balaguer N., Popoola O., Broday D., Martinez-Iñiguez T., Nieuwenhuijsen M., Jovasevic-Stojanovic M., Topalovic D., Jones R.L., Galea K., Etzion Y., Kizel F., Golumbic Y., Baram-Tsabari A., Robinson J., Kocman D., Horvat M., Svecova V., Arpaci A., Bartonova A., An evaluation tool kit of air quality micro-sensing units. Science of the Total Environment, 2016. doi.org/10.1016/j.scitotenv.2016.09.061.

Gao R.S., Telg H., McLaughlin R.J., Ciciora S.J., Watts L.A., Richardson M.S., Schwarz J.P., Perring A.E., Thornberry T.D., Rollins A.W., Markovic M.Z., Bates T.S., Johnson J.E., Fahey D.W., A light-weight, high-sensitivity particle spectrometer for PM2. 5 aerosol measurements. *Aerosol Science and Technology,* 50(1):88-99, 2016.

Hasenfratz D., Saukh O., Walser C., Hueglin C., Fierz M. Deriving High-Resolution Urban Air Pollution Maps Using Mobile Sensor Nodes. 2014, 1–25.

Kanaroglou P., Jerrett M., Morrison J., Bernardo Beckerman M., Arain A., Gilbert N., Brook J., Establishing an air pollution monitoring network for intra-urban population exposure assessment: a location-allocation approach. *Atmos. Environ.,* 39(13):2399–2409, 2005.

Lerner U., Yacobi T., Levy I., Moltchanov S., Cole-Hunter T., Fishbain B., The effect of ego-motion on environmental monitoring. Science of the Total Environment 533:8–16, 2015.

Mead M., Popoola O., Stewart G., Landshoff P., Calleja M., Hayes M., Baldovi J., McLeod M., Hodgson T., Dicks J., Lewis A., Cohen J., Baron R., Saffell J., Jones R., The use of electrochemical sensors for monitoring urban air quality in low-cost, high-density networks. Atmospheric Environment, 70:186-203, 2013.

Moltchanov S., Levy I., Etzion Y., Lerner U., Broday D.M., Fishbain B., On the feasibility of measuring air pollution at dense urban areas by wireless distributed sensor networks. Science of the Total Environment, 502:537–547, 2015.

Sabaliauskas K., Jeong C.H., Yao X, Evans G.J., The application of wavelet decomposition to quantify the local and regional sources of ultrafine particles in cities. *Atmos. Environ.*, *95:*249–257, 2014.

Stetter J.R., Li J., Amperometric gas sensors a review. Chemical reviews, 108(2):352-366, 2008.

Ulanowski J., Kaye P., Hirst E., Wieser A., Stanley W., Miniature, low-cost optical particle counters. In *Int. Conf. Optical Characterization of Atmospheric Aerosols*, Smolenice, Slovakia, 2013.

Yu C.H., Fan Z.-H., Lioy P.J., Baptista A., Greenberg M., Laumbach R.A. Novel mobile monitoring approach to characterize spatial and temporal variation in traffic-related air pollutants in an urban community. *Atmos. Environ.*, *141:*161–173, 2016.

Yuval, Broday D.M., Studying the time scale dependence of environmental variables predictability using fractal analysis. Environmental Science and Technology, 44(12):4629–4634, 2010.

